Dehydration of Hydrazine Hydrate by Pervaporation: Blending of Polymers, Modification and Characterization of Membranes.

By
Mr. Sukalyan Dutta

to the

Department of Chemical Engineering

INDIAN INSTITUTE OF TECHNOLOGY KANPUR

August, 2004

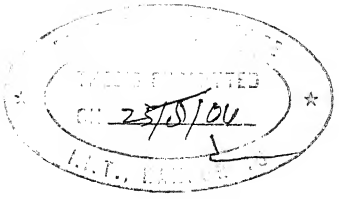

CERTIFICATE

This is to certify that the thesis entitled "Dehydration of Hydrazine hydrate by pervaporation: Blending of polymers, modification and characterization of membranes" is the original work of Mr. Sukalyan Dutta carried out under my supervision, and it has not been submitted elsewhere for a degree.

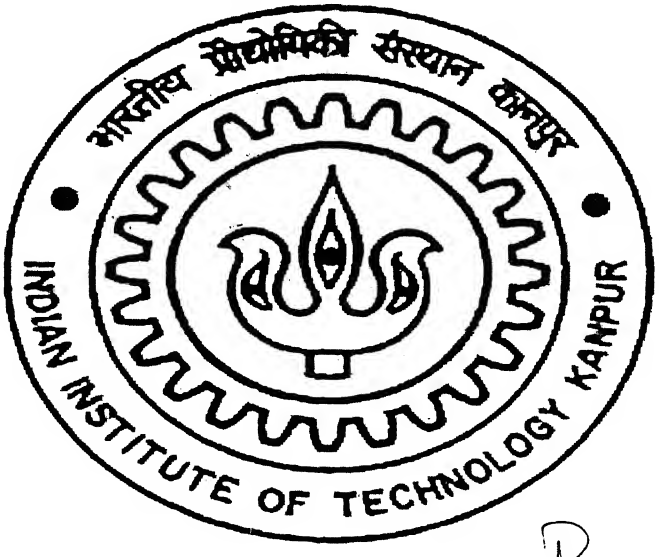

Dr. P.K. Bhattacharya
Professor
Dept. of Chemical Engineering
IIT Kanpur
Kanpur – 208016

25th **August, 2004**

Dedicated
to
Open Source Community

Use Linux

ABSTRACT

Anhydrous hydrazine is an important inorganic compound used for space program as rocket propellant. However, hydrazine hydrate is commercially obtained at 64 wt% (as it is coming out from ordinary distillation). Anhydrous hydrazine, therefore, is usually obtained by breaking the azeotrope (71.5 wt% hydrazine) by a third component which further causes problems. Needless to mention, such conventional separation processes require high energies. Pervaporation is a process known to find its utility for such cases and hence can be an alternative process. However, the process heavily depends upon the selection of polymer(s) in the form of membrane. Further, in the case of hydrazine hydrate separation alkalinity plays an important role for the efficient selection of polymer(s).

Various polymeric membranes (laboratory prepared) were chosen as candidate materials for hydrazine hydrate separation studies. Acrylo-nitrile butadiene styrene (ABS) was chosen as the principle polymer which was further blended with ethyl cellulose. Characterizations of these blended membranes (through measurement of contact angles, XRD, positron annihilation, FTIR, etc.) were done for such blended membranes (varying ratios on weight basis).Sorption studies was also carried out to measure equilibrium sorption. Polystyrene (PS) is also being sulphonated using various dosages and concentrations of sulphuric acid. Further, these membranes were characterized using FTIR technique.

The separation of hydrazine hydrate by pervaporation was one of the key components of assessing the performances of such blended/modified membranes. Experiments are being carried out in a laboratory developed experimental rig with advanced instrumentations to observe flux and selectivity of various such prepared membranes based on a fixed set of operating conditions (temperature: 50°C, pressure: 0.1mmHg, static feed condition).

Acknowledgements

It was highly eventful at the **Department of Chemical Engineering**, IIT Kanpur, working with a dedicated community, which I will cherish throughout my life. During the research work, my thesis guide **Prof. P. K. Bhattacharya** has helped me immensely with his ingenious ideas and valuable guidance. I am highly grateful to him for motivating and encouraging me at all the stages of my thesis work. By working under his auspices I have come to know the intricate details of research work. His guidance will act as beacon of light throughout my life.

I would also like to thank **Dr. S. V. Satyanarayana** for the spirit he incited in our lab for "Pervaporation". Without his constant support, valuable suggestions, and particularly, the immediate resolutions to my queries, it would have not been possible for me to land at this stage.

I shall always cherish the sweet memories attached with my lab mates, **Mrinal, Sumesh, Prince, Rakhi, Ravi, Satish, Gagan**. They have always helped to maintain a friendly atmosphere in our lab. More than this they have been a constant source of inspiration. A thank is due to the lab assistant **Mr. Nagendra and Mr. Ramesh Chandra** for their help.

I am especially thankful to all those wonderful friends, **Prakash, Debu, Subhashis, Rudra, Manoj** and **Phugal** for the wonderful time we spent in hall-4. The memories associated with them will surely be cherished forever.

At the end I would like to convey regards to my parents and all other family members. Their silent presence behind my all achievements cannot be properly expressed.

The chain of my gratitude would be definitely incomplete if I would forget to thank the first cause of this chain, using Aristotle's words - "The Prime Mover". I thank "**The Almighty**" for just one thing and that is- "Everything".

25th August 2004 *Sukalyan*

Contents

List of figures

List of Tables

Nomenclature and Abbreviations

1. Introduction

1.1 Pervaporation Process 1

1.1.1 Types of Pervaporation 3

1.1.2 Membranes used 5

1.2 Hydrazine Hydrate Separation 5

1.3 Objectives 7

2. Literature Review

2.1 Pervaporation 8

2.2 History 9

2.3 Applications 10

2.4 Merits and Limitations of Pervaporation 12

2.5 Mass Transport Models of Pervaporation 12

2.5.1 Solution-Diffusion Model 12

2.5.2 Pore Flow Model 14

2.5.3 PPCSD Model 15

2.6 Pressure Profile and Location of Vaporization 16

3. Theoretical

3.1 Pervaporation -Process definition 18

3.2 Chemical Potential and Activity 19

3.3 Mass Transport within the Membrane and Membrane selection 20

3.4 Characterization Methods 23

3.4.1 Contact Angle 23

3.4.2 X-Ray Diffraction (XRD) 24

3.4.3 Fourier transform infrared spectroscopy 25

3.4.4 Positron annihilation lifetime spectroscopy (PAS) 25

4. Experimental

4.1 Materials and Chemicals 28

4.2 Instruments and other auxiliary accessories 28

4.3 Preparation of membrane 29

4.3.1 Polymer solution 29

4.3.2 Blending 29

4.3.3 Casting 30

4.3.3 Modification of polymer 30

4.4 Membrane density: Measurements 31

4.5 Contact Angle Measurements 32

4.6 Sorption 32

4.7 Analysis 32

4.8 Pervaporation: Set up and Procedure 33

5. Results and Discussion

5.1 Separation study of blended ABS & EC membranes 36

5.1.1 Influence of ABS composition in blended membrane on Flux 37

5.1.2 Influence of ABS composition (on membrane) on Selectivity and PSI index 42

5.2 Characterization of blended membranes 48

5.2.1 XRD 48

5.2.2 Positron Annihilation Lifetime (PAL) Spectroscopy 54

5.2.3 Contact angle analysis 55

5.3 Sorption study of blended ABS & EC membranes 59

5.3.1 Pure component sorption 59

5.3.2 Binary component sorption 59

5.4 Separation study of Modified PS membranes 62

5.4.1 Influence sulphonation in modified membrane on Flux 62

5.4.2 Influence of sulphonation in modified membrane on selectivity & PSI index 66

5.5 Characterization of modified membranes using FT-IR technique 70

6. Conclusions **73**

Appendix 76

References 88

List of Figures

1.1 Schematic diagram of liquid permeation through dense membranes 4

2.1 Schematic diagram of industrial pervaporation set up 11

2.2 Schematic representation of Solution Diffusion Mechanism 13

2.3 Schematic representation of Pore Flow Model 14

2.4 Schematic description of pseudophase change solution-diffusion (PPCSD) model 16

3.1 Schematic diagram of Pervaporation Process using Vacuum or Carrier gas 18

3.2 Solubility parameter diagram of PPN/CA alloy membrane α - Separation Factor for the azeotropic composition
PPN: Poly-phosphonate CA: Cellulose acetate 22

3.3 Contact Angle θ, made by a liquid on a solid surface 23

3.4 Typical diffraction pattern in lattice planes, Bragg's law 24

4.1 Reaction between Polystyrene and Sulphuric acid 31

4.2 Schematic diagram of the experimental setup for pervaporation 34

5.1 Flux values for different blended membranes 39

5.2 Normalized Flux $(J)_I$ variation with varying composition of ABS polymer in EC polymer for blended membranes 40

5.3 Normalized Flux $(J)_{II}$ variation with varying composition of ABS polymer in EC polymer for blended membranes 41

5.4 Effect of percentage of ABS in blended membrane on selectivity 45

5.5 $(PSI)_I$ index values obtained for blended membranes 46

5.6 Variation of $(PSI)_{II}$ index with varying composition of ABS in blended membranes 47

5.7 XRD spectrum of ABS membrane 49

5.8 XRD spectrum of BABS1 membrane 50

5.9 XRD spectrum of BABS2 membrane 51

5.10 XRD spectrum of BABS3 membrane 52

5.11 XRD spectrum of BABS5 membrane 53

5.12 Variation of contact angle for varying composition of ABS in blended membranes 57

5.13 Variation of Selectivity for varying contact angles (water) 58
5.14 Sorption of water as a function of time for blended membranes 60
5.15 Sorption of hydrazine hydrate as a function of time for blended membranes 61
5.16 Flux for different sets of modified membranes obtained with varying concentration of H_2SO_4 64
5.17 Normalized Flux for different sets of modified membranes obtained with varying concentration of H_2SO_4 65
5.18 Selectivity for different sets of modified membranes obtained with varying concentration of H_2SO_4 68
5.19 PSI index for different sets of modified membranes obtained with varying concentration of H_2SO_4 69
5.20 FTIR spectrum of MPS4 membrane 71
5.21 FTIR spectrum of MPS4 membrane (3000 -2000 cm^{-1}) 72
A.1 G.C Calibration of hydrazine hydrate system 76

List of Tables

4.1 Composition along with notations of blended membranes 30
4.2 Composition along with notations of modified PS membranes 31
5.1 Experimental and normalized values of flux obtained for blended membranes along with the properties 38
5.2 Selectivity and PSI indexes for membranes 43
5.3 Positron annihilation parameters and respective free volume parameters of blended membranes 55
5.4 Values of Contact angles of water on different membranes 55
5.5 Experimental results for sorption of water and hydrazine hydrate 59
5.6 Experimental and normalized values of flux obtained for sulphonated PS membranes along with thickness 62
5.7 Selectivity and PSI indexes for membranes 66
A.2: Table for plotting G.C. calibration curve 77
B.1:Flux and selectivity as a function of time for a feed concentration of 64% Hydrazine Membrane used –EC 78
B.2:Flux and selectivity as a function of time for a feed concentration of 64% Hydrazine Membrane used –BABS1 78
B.3:Flux and selectivity as a function of time for a feed concentration of 64% Hydrazine Membrane used –BAB2 79
B.4:Flux and selectivity as a function of time for a feed concentration of 64% Hydrazine Membrane used –BAB3 79
B.5:Flux and selectivity as a function of time for a feed concentration of 64% Hydrazine Membrane used –BAB4 79
B.6:Flux and selectivity as a function of time for a feed concentration of 64% Hydrazine Membrane used –BAB5 80
B.7:Flux and selectivity as a function of time for a feed concentration of 64% Hydrazine Membrane used –ABS 80

B.8:Flux and selectivity as a function of time for a feed concentration of 64% Hydrazine Membrane used – MPS0 81

B.9:Flux and selectivity as a function of time for a feed concentration of 64% Hydrazine Membrane used – MPS1 81

B.10:Flux and selectivity as a function of time for a feed concentration of 64% Hydrazine Membrane used – MPS2 81

B.11:Flux and selectivity as a function of time for a feed concentration of 64% Hydrazine Membrane used – MPS3 82

B.12 :Flux and selectivity as a function of time for a feed concentration of 64% Hydrazine Membrane used – MPS4 82

C.1: Table for calculating membrane density 83

C.2: Table for membrane density & membrane thickness 83

D.1: Variation of percentage sorption of water on different blended membrane 84

D.2: Variation of percentage sorption of Hydrazine hydrate on different blended membrane 84

D3: Major XRD intensity data's for various membranes

D3.1: Membrane –ABS 84

D3.2: Membrane –BABS1 85

D3.3: Membrane –BABS2 86

D3.4: Membrane –BABS3 86

D3.5: Membrane –BABS5 87

Nomenclature

a_i	activity of substance *i*
c_i	mass concentration of *i*
c_m	mass concentration of *m*
C_{1m} & C_{2m}	WLF constants
d_{eff}	effective diameter
D_{im}	mutual diffusion coefficient of *i* in *m* (m^2/s)
i	liquid component
J	mass flux of ($kg/m^2.h$)
J_m	mass flux of *m*, ($kg/m^2.h$)
J_{iD}	diffusional mass flux ($kg/m^2.h$)
k	Boltzmann constant (1.38048×10^{-23} J/K)
m_i	thermodynamic diffusion coefficient or mobility
M_c	average molecular weight between two cross links
M_i	molecular weight of *i*
p	pressure
p_f	feed side pressure
p_d	downstream side pressure
p_e	Kelvin vapour pressure of permeating liquid
p_s	saturation vapour pressure of the permeating liquid
r	pore radius
R	Universal Gas constant
S_c	contactable surface area
S_{im}	spreading coefficient
T	absolute temperature
T_g	glass transition temperature
v_i	molal volume at the normal boiling point
$\hat{v}_i^*$ and $\hat{v}_m^*$	specific hole free volume for *i* and *m*
$\tilde{v}_m$	Partial specific volume of the membrane
V_i	permeating liquid molar volume

$\tilde{V}_c$	solvent's critical molar volume
$\hat{V}_i$	specific volume of the pure solvent
V_{eff}	effective molecular volume
w_i	weigh fraction of solvent
w_m	weigh fraction of polymer
x_i	mole fraction of component
l	thickness of the mebrane

Greek letters

ρ	density of membrane
γ_{mi}	interfacial tension between solid and liquid
γ^{LW},	aploar of Lifshitz van der Waals (LW) component
γ^{+}	electron acceptor surface tension component
γ^{-}	Electron donor surface tension component
δ_v	thickness of the membrane for vapour transport
δ_t	total thickness of the membrane
ζ^*	value of ζ in the reference state
η_i	viscosity of the pure solvent
θ	contact angle
μ_i	chemical potential of *i*
μ_i^o	standard chemical potential
ξ	ratio of the molar volume of a solvent jumping
ρ_m	polymer density
ρ_i	solvent density
χ	Flory-Huggin's interaction parameter
φ	Association factor
ϕ_m	Volume fraction of membrane
ϕ_i	Volume fraction of permeating liquid
δ_p	polar forces of attration
δ_h	hydrogen bonding force of attraction

Suffix

A	preferentially pervaporated species
B	less pervaporated species
‘	feed side
“	permeate side
atm	atmospheric
air	air

Abbreviation

PV	pervaporation
PDMS	polydimethylsiloxane
PVA	polyvinyl alcohol
PPN	Poly-phosphonate
CA	Cellulose acetate
XRD	X-Ray diffraction
FT-IR	Fourier transform infrared spectroscopy
WAXRD	Wide angle X-Ray diffraction
PSI	Pervaporation selective index
PAL	positron annihilation technique

Chapter 1

Introduction

Hydrazine is an important inorganic chemical with high heats of combustion and hence becomes candidate material for rocket fuels. The other main applications of hydrazine include de-oxygenation of boiler feed water, fuel cells and production of blowing agents. However, production of hydrazine which is carried out using any of the known various reaction routes still pose problems with regard to its yield and purity [1]. Ordinary distillation provides hydrazine in the form of hydrate (64% by wt of hydrazine). This form of hydrazine finds wide applications; whereas, use of hydrazine in rocket propulsion requires in the form of anhydrous hydrazine. Therefore, removal of water from hydrate state to produce anhydrous hydrazine is essential and to make it suitable for such purposes. However, conventional separation techniques for the removal of water experience difficulty as hydrazine forms an azeotrope with water at 71.5 wt % of hydrazine [2]. Further, hydrazine and water are highly polar substances (surface tension values very close) and between them there is strong hydrogen bonding. Therefore, conventionally, combinations of processes are required to seek dehydration. These are chemical reactions, followed by distillation or azeotropic distillation with aniline as entrainer. Hydrazine also poses a dangerous fire and explosion risk and can explode during distillation if traces of air are present, apart from other limitations like high energy consumption and cost. Hence, there is a need to search alternative technologies to produce anhydrous hydrazine. Application of membrane technology is one such attempt to address the stated problems [3-5]. Pervaporation process, in particular, may be examined because of its potential to separate azeotropic mixtures.

1.1 Pervaporation Process

Pervaporation, in its simplest form, is an energy efficient process combining membrane permeation and evaporation processes. Pervaporation involves the separation of two or more components across a membrane by differing rates of diffusion through a

thin polymer film and an evaporative phase change comparable to a simple flash step. A concentration and vapor pressure gradient is used to allow one component to preferentially permeate across the membrane. The permeated product (pervaporate) is removed as vapour by màintaining the downstream pressure lower than the saturation pressure in the downstream side [6]. The components in the liquid stream getting sorbed into the membrane and then permeate through the membrane. The permeating molecule finally changes into its vapour as and when its meets pressure lower than its corresponding condition (either within the membrane or just outside the membrane at the downstream side). The sizes of the molecules that need to be separated are in the same order of magnitude. Thus, nonporous membranes are employed whereas porous membranes do not function effectively. Further, the mass flux may be affected by maintaining the downstream pressure much lower than the saturation pressure at the prevailing condition. Such a low pressure can be achieved either employing a carrier gas or using a vacuum pump at the downstream side. The membrane acts as a thin solvent layer and the pervaporate composition is mainly governed by the preferential solvation of the polymeric barrier material. As a result, the liquid-vapour equilibrium is greatly perturbed.

The mass transport of permeate through a pore free perm-selective film involves three successive steps:

i. Upstream partitioning of the feed-components between the flowing liquid mixture and the swollen upstream layer of the membrane,
ii. Diffusion of the penetrants through the unevenly-swollen permselective barrier, and
iii. Vapour phase desorption at the downstream surface of the film.

This multi-step process is evidently much more complex and it is easily understandable that the composition of the pervaporate may widely differ from that of the mixed vapour evolved after the establishment of free liquid-vapour equilibrium. The use of an appropriate membrane generally makes it possible to efficiently separate a number of binary azeotropic mixtures.

The permeability of liquids through polymeric membranes can be considered as the product of solubility and diffusion coefficient. Liquid mixtures with similar diffusion

coefficients can be separated if solubilities are different and vice versa; or separation can be a result of combination of both parameters.
Pervaporation is typically suited to separating a minor component of a liquid mixture, thus high selectivity through the membrane is essential. Figure 1.1 shows an overview of the pervaporation process.

Pervaporation can be used for breaking azeotropes, dehydration of solvents, organic/organic separations and removal of other volatile organics such as ethanol/methanol dehydration and wastewater purification. Characteristics of the pervaporation process include:

1. Low energy consumption
2. No entrainer required, no contamination
3. Permeate must be volatile at operating conditions
4. Functions independent of vapor/liquid equilibrium

1.1.1 Types of Pervaporation

Batch pervaporation is a simple system with great flexibility; however, a buffer tank is required for batch operation. Continuous pervaporation consumes very little energy and operates effectively with low impurities in the feed. Further, it is much useful with larger capacities. Vapor phase permeation is preferred for direct feeds from distillation columns or for streams with dissolved solids.

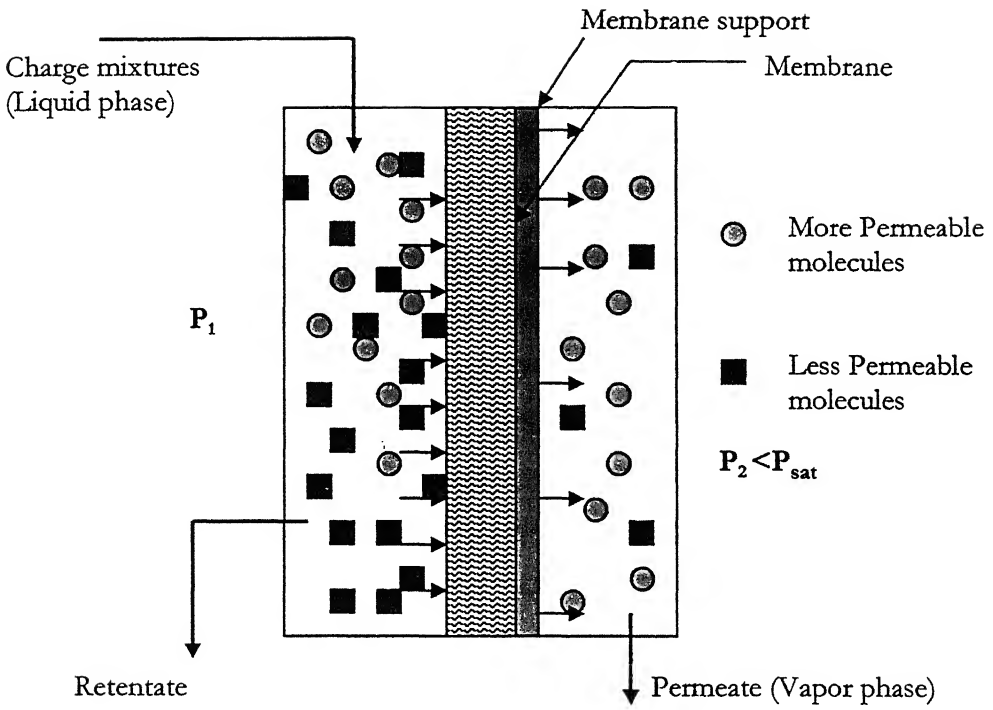

igure1.1 Schematic diagram of liquid permeation through dense membranes

1.1.2 Membranes used

The membranes used in pervaporation processes are classified according to the ıature of the separation being performed. Hydrophilic membranes are used to remove vater from organic solutions. These types of membranes are typically made of polymers vith glass transition temperatures being greater than room temperatures. A polymer like ›olyvinyl alcohol is an example of a hydrophilic membrane material. Organophilic nembranes are used to recover organics from solutions. These membranes are typically nade up of elastomeric materials (polymers with glass transition temperatures below oom temperature). The flexible nature of these polymers makes them ideal for allowing ›rganics to pass through. Examples of these organophilic materials include nitrile, ›utadiene rubber, and styrene butadiene rubber.

.2 Hydrazine Hydrate Separation

Hydrazine, being explosive by nature, poses problems to purify hydrazine from vater (from hydrazine - water system) through high temperature distillation. Thus mbient temperature operation of pervaporation is of significance for the use of hydrazine -water system. The selection of polymer for hydrazine separation plays an important role lue to high alkaline nature of hydrazine (pH>12.5) and only few polymers are available hat may withstand such high alkalinity. Further, hydrazine has strong reducing and ıydrolyzing effects. Ravindra et al. [5] have used ethyl cellulose (EC) membrane to carry ›ut this separation. Even though, ethyl cellulose is highly selective for water at low oncentrations of hydrazine, it, however, gives low selectivity for 64% aqueous ıydrazine solution. Further, it was reported that ethyl cellulose is selective for hydrazine luring sorption and selective for water during diffusion [7].

Therefore, such a problem may be addressed by selecting a membrane with high vater-permselectivity. This may be achieved by increasing the sorption selectivity (water ɔ hydrazine) or diffusion selectivity. For a better sorption ratio, hydrophilic moiety may ›e introduced into the polymer chain to enhance water sorption but hydrazine sorption

may also increase because of high polarity of the compound. In addition to this, excessive swelling may decrease diffusion selectivity because of increase in free volume and overall selectivity which may further decrease [8]. Various hydrophilic chitoson and modified chitoson membranes were previously used [9] and were found to have low selectivities. Again for better diffusion ratio, the hydrophobic moiety may be introduced into the polymer chain. This may, however, decrease permeation rate. Thus, with the introduction of balanced quantities of hydrophilic and hydrophobic moieties better flux and better selectivity may be obtained. In this regard, one may combine the properties of hydrophilic and hydrophobic polymers while casting a membrane and may thus achieve high values of flux and selectivity.

In this regard, a new polymer, acrylonitrile butadiene styrene (ABS) was utilized for its properties of both hydrophilic and hydrophobic. The present work, therefore, contemplates to combine (by blending) ethyl cellulose (hydrophilic) and ABS polymers in different proportions. Further, in this regard, modification of hydrophobic polystyrene (PS) polymer is also contemplated by introducing sulphonic groups (through sulphuric acid reaction) to increase hydrophilicity of the polymer. This approach was earlier utilized in a recent work [10] where ethyl cellulose polymer was modified by introducing carbamate groups (reacting ethyl cellulose with phenyl iso-cyanate) to increase hydrophobicity of the polymer.

It is, therefore, decided to examine separation by pervaporation process at fixed operating conditions (temperature: 50°C, downstream pressure: 0.1mmHg, static feed condition) using laboratory prepared membranes (ABS blended with ethyl cellulose, modified polystyrene). Further, in order to characterize such modified membranes their pore size as well as surface characteristics was examined. Experimental investigations were also planned to observe flux and selectivity utilizing these modified membranes. Modifications were also based on degree of sulphonation which were studied through pervaporation flux and selectivity.

3 Objectives

ısed on the above discussion the following broad objectives were laid down:

i. Blending of ABS and EC polymer by varying weight percentages.
i. Modification of PS polymer by introducing sulphonic groups in the polymer chain through the reaction with sulphuric acid.
i. Experimental studies of dehydration of hydrazine hydrate (64 wt %) using these various blended and modified membranes.
/. Characterization of blended and modified membranes using positron annihilation (PAL) technique, XRD, FTIR and Contact angles.

Chapter 2

Literature Review

Separation processes play an important role in the chemical industries for purifying raw materials, recovering product streams of desired purity and preventing pollution through treatment of waste streams released to the environment. It was estimated that around 30-70% of the capital cost of the chemical industry is accounted by separation processes [11]. The national research council reported more than 50 different types [11] of separation processes, including membrane based separations. Membrane processes are already well known for its relevance in the water desalination, effluent treatment, food processing, medical applications, gas separations and liquid mixture separations, etc. Membrane processes are classified with respect to the use of membranes (homogeneous or microporous), types of driving forces (difference of pressure, concentration, etc.) and nature of feed solutions (ionic, non-ionic, liquid, gas, etc.). Reverse osmosis, ultrafiltration, nanofiltration, microfiltration are pressure driven processes. Gas separation and pervaporation are other recently developed processes. An attempt has been made, in the present thesis, to understand basic transport mechanism and the nature of the membrane behind newly evolved membrane separation processes of pervaporation. The following paragraphs, therefore, touch upon the basic phenomena and principles of the process to illustrate the intricacies involved in the process.

2.1 Pervaporation

Pervaporation is a process in which a liquid mixture is separated into its components by virtue of employing a selective (dictated by solubility) membrane. The name pervaporation in itself indicates the permeation and vaporization through the membrane. The separation is carried out using a dense or homogeneous film. The feed solution to be separated is contacted on one side of the membrane and the permeate, in vapour form, is obtained on the other side of the membrane by applying pressure lower than the saturation vapour pressure. The concentration gradient across (and within) the

membrane is the driving force for the mass transport. This can be achieved by keeping the other side under dry state as compared to the feed side which is always kept under wet state. Usually, either vacuum (vacuum pervaporation) is applied or an inert gas (sweeping gas pervaporation) is passed on the other side. Besides these two modes of operation, there are several other process variants, including thermo pervaporation [12], vapour permeation [13], vacuum aided reverse osmosis [14], perstraction [15], membrane distillation [16,17], and electrically induced pervaporation [18].

Unlike other membrane processes, pervaporation involves a phase change of permeate. Therefore, the enthalpy of vaporization is the minimum amount of energy required for the process. Further, there is strong interaction between liquid feed components and membrane, resulting into high swelling of membrane. The swelled film works as a pseudo-liquid immobilized layer. Further, swelling tends to alter the membrane properties and generally leads to higher permeability and lower selectivity. The swelled membrane allows the diffusion of feed components from one side of the membrane to other. Thus, the permeate composition is mainly determined by relative affinities of the feed components and also for their unequal mobilities within the membrane. Accordingly, permeate composition varies from that of the vapour liquid equilibrium [19].

2.2 History

The phenomenon of pervaporation was first observed by Kober [20] for his experiments on evaporation of water placed in a collodion (cellulose nitrate) bag into atmospheric air. Before to this, in 1906 Kahlenberg [21] reported some qualitative observations concerning the selective transport of hydrocarbon/alcohol mixtures through a thin rubber sheet. In 1935, Farber [22] recognized the usefulness of pervaporation for separation and concentration. However, Heisler et al. [23] reported the first quantitative work for the separation of alcohol/water using cellulose film by pervaporation. Binning and co-workers [24,25] carried out pervaporation of different mixtures and highlighted the potential application of pervaporation. A first commercial application of pervaporation, installed in Brazil, was reported in 1982 [26] for the separation of alcohol-water mixtures using G.F.T. (Gesellschaft für Trenntechnik, Homburg/Saar, F.R.G)

membrane. Meanwhile, development of new membranes, experimental investigations, fundamental understandings, theoretical models, and module designs are in progress [27, 28].

2.3 Applications

Pervaporation finds several applications and may be classified into various categories as:

1. *Dehydration of liquid mixtures*; a) Azeotropic mixtures: Ethanol – water, Dioxane – water, etc.; b) Close boiling mixtures: acetic acid – water; c) Electrolytic solutions.
2. *Removal of organics from water*; a) Pollution control: toluene-water, benzene-water, etc.; b) Aroma recovery: apple juice aroma compounds, etc.; c) Wine and beer dealcoholisation.
3. *Separation of organic –organic mixtures*; a) Azeotropic mixtures: Benzene – cyclohexane, MTBE – methanol, etc.; b) Isomers: C8 isomers.
4. *Reactive pervaporation*; Removal of water from the product of esterification reactions to shift equilibrium reaction towards the product side.
5. *Hybrid process*; integrating pervaporation unit with other conventional units.

A schematic diagram of industrial pervaporation process set up is shown in Figure 2.1. Industrial applications of pervaporation include separation or purification of following products.

Alcohols	**Ketones**
Methanol	Acetone
Ethanol	Butanone
Propanol (both isomers)	Methyl isobutyl ketone (MIBK)
Butanol (all isomers)	**Amines**
Pentanol (all isomers)	Triethylamine
Cyclohexanol	Pyridine
Benzyl alcohol	Aniline
Aromatics	**Aliphatics**

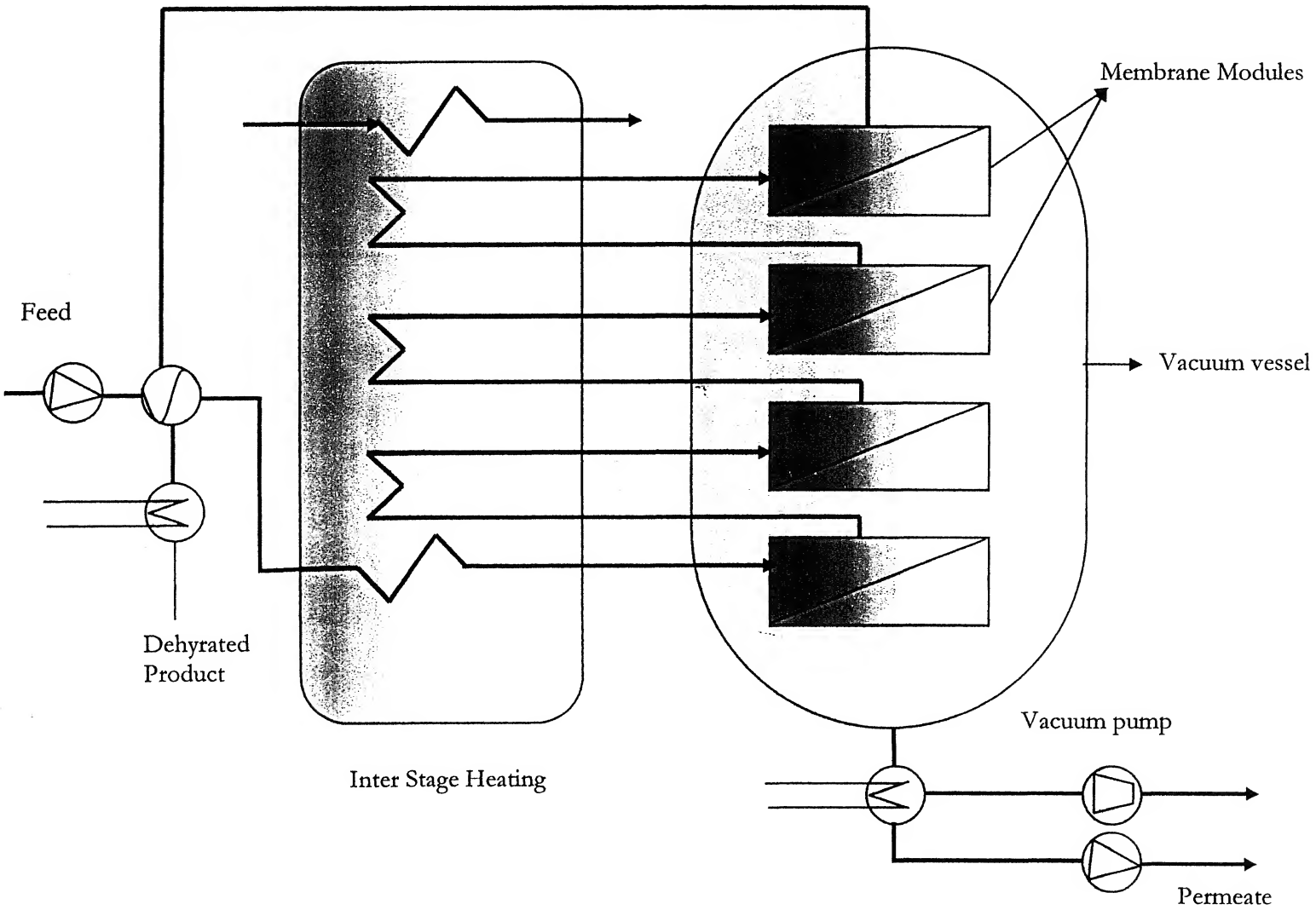

Fig 2.1 Schematic diagram of industrial pervaporation set up

Benzene	Chlorinated hydrocarbons (various)
Toluene	Dichloro methane
Phenol	Perchloroethylene
Ester	**Ethers**
Methyl acetate	Methyl tert-butyl ether (MTBE)
Ethyl acetate	Ethyl tert-butyl ether (ETBE)
Butyl acetate	Di-isopropyl ether (DIPE)
Organic Acid	Tetrahydro furan (THF)
Acetic acid	Dioxane

2.4 Merits and Limitations of Pervaporation

It is being considered that in addition to various applications, pervaporation may be energy efficient, pollution free, easier plant installation, maintenance, and expansion. Bravo et al. [29] ranked pervaporation third highest amongst the 31 techniques under evaluation for the fluid separation. Further, in 1983, Baker [30] had predicted that by the year 2000 all the refineries would have used pervaporation for the separation of liquid mixture. The process, however, could not fulfill its earlier promise because of low flux with dense membranes, low selectivity due to high swelling of the membrane, lack of mathematical models, lack of design of high compact modules, lack of cost estimations, fundamental understandings (particularly downstream pressure effect), etc.

2.5 Mass Transport Models of Pervaporation

A well established mass transport model is essential for engineering membranes separation processes. Unlike other membrane separation processes, mass transport through a pervaporation membrane process involves more complicated physiochemical interactions between permeants and the membrane. Several approaches have been proposed to describe the process.

2.5.1 Solution-Diffusion Model

The solution-diffusion model is accepted by the majority of membrane researchers [31].

According to this mechanism, pervaporation consists of three consecutive steps:

i. Sorption of the permeant from the feed liquid to the membrane,

ii. Diffusion of the permeant on the membrane, and

iii. Desorption of the permeant to the vapor phase on the downstream side of the membrane.

It is illustrated in Fig 2.2. In general, solubility and diffusivity are concentration dependent. A number of mathematical equations for mass transport have been formulated on the basis of Fick's diffusion equation using different empirical expressions of concentration dependence of solubility and/or diffusivity. However, these equations cannot be taken for granted unless they are used within the experimentally established range for which the relationships expressed for diffusion and thermodynamic equilibria are applicable.

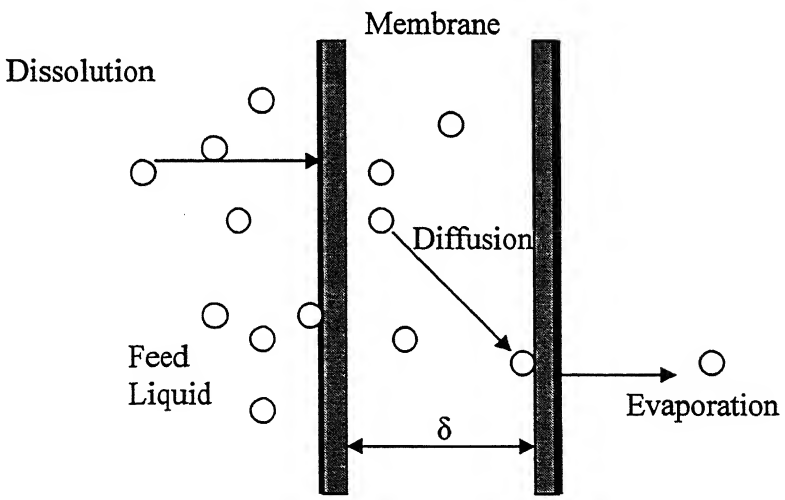

Figure 2.2 Schematic representation of Solution Diffusion Mechanism

Assuming that the diffusivities of individual permeants are proportional to the total concentration of permeants in the membrane, Green law et al [31] presented a simple model. However this model does not apply to nonideal cases such as alcohol water mixtures. On the same basis, a "six-coefficient exponential model" was proposed

[32], but the significance of model parameters become suspect, and the model is of little predictive of interpretive. A more complex model was presented taking into consideration of the coupling effects on both sorption and diffusion. This model supposes the knowledge of diffusivity as a function of concentration, which is in fact one of the most difficult problems yet to solve in mechanistic approach. An alternative approach based on an extension of the free-volume theory for diffusion in polymers was pursued later. Then it was modified by introducing the interaction parameters on the basis of Flory-Huggins thermodynamics and the effects of flux coupling [33].To facilitate mathematical treatment a different approach was presented [34], considering pervaporation as combination of liquid evaporation and vapor permeation. The normal solution diffusion model was simply applied to describe vapor permeation. But it was proved that this is not the case under any circumstances. Although, confirmations of solution-diffusion model have been accumulated for various boundary conditions; studies dealing specifically with the influence of downstream pressure on pervaporation fluxes are exceptions and remain somewhat controversial. The conspicuous unconcern of phase change in this explanation poses some questions.

2.5.2 Pore Flow Model

Recently a transport model was proposed on the basis of the pore flow mechanism [35]. It is assumed that there are a bundle of straight cylindrical pores on the membrane.

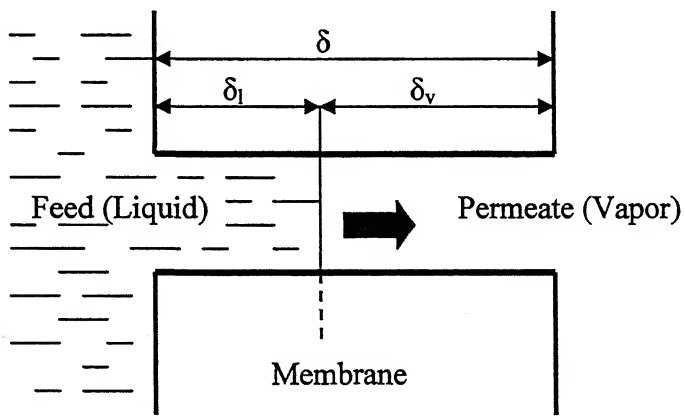

Figure 2.3 Schematic representation of Pore Flow Model

The mass transport by pore flow mechanism also consists of three steps:

i. Liquid transport from the pore inlet to a liquid-vapor phase boundary,
ii. Evaporation at the phase boundary, and
iii. Vapor transport from the boundary to the pore outlet.

It is illustrated in Figure 2.3. In consideration that (i) the physical structure of the membrane is accounted for explicitly in the pore flow model, (ii) the position of the phase change of permeant in the membrane is clearly addressed in the pore flow model, (iii) several main features of pervaporation observed experimentally can be explained semi quantitatively by the pore flow model , and (iv) good models that enable description and prediction of pervaporation transport are still lacking, the pore flow model should be appreciated, although the present quantitative expression of the pore flow model is at a preliminary stage because some macroscopic concepts such as viscosity and friction constant are used in the derivation of the model equations, while fluid continuity does not necessarily hold when the pores are very small. Moreover the extensions of this model take into account of the vapour-liquid equilibrium data, without considering the change in vapor pressure itself with in a pore.

2.5.3 PPCSD Model

Using assumptions of thermodynamic equilibrium, simple concentration-dependent solubility, and diffusivity, a set of analytical equation were derived to express the pervaporation flux [36], which is called pseudophase-change solution diffusion model or PPCSD model. It assumes pervaporation is a combination of liquid permeation and vapor permeation mechanism in series. This is illustrated in figure 2.4. A pseudophase of permeant is located at the interface between these two mechanisms. The resultant equations were similar to that of pore flow model. This model was tested for its validity and showed good agreement with literature data in terms of the effect of feed pressure and permeate pressure. Comparison among three different membrane separation processes (namely, pervaporation, vapor permeation, liquid permeation) showed that the permeation flux is nearly same for pervaporation and vapor permeation processes under the assumption of thermodynamic equilibrium. On the other hand, the permeation flux for

the liquid permeation process is always lower unless a certain high feed pressure is reached. But the assumption of pseudophase inside the membrane with same and simple relations of solubility and diffusivity holding for vapor and liquid permeation mechanisms is questionable. In liquid permeation zone, activity gradient is neglected, while for vapor, pressure contributions are neglected. Moreover the parameters used are assumed to be same in both zones.

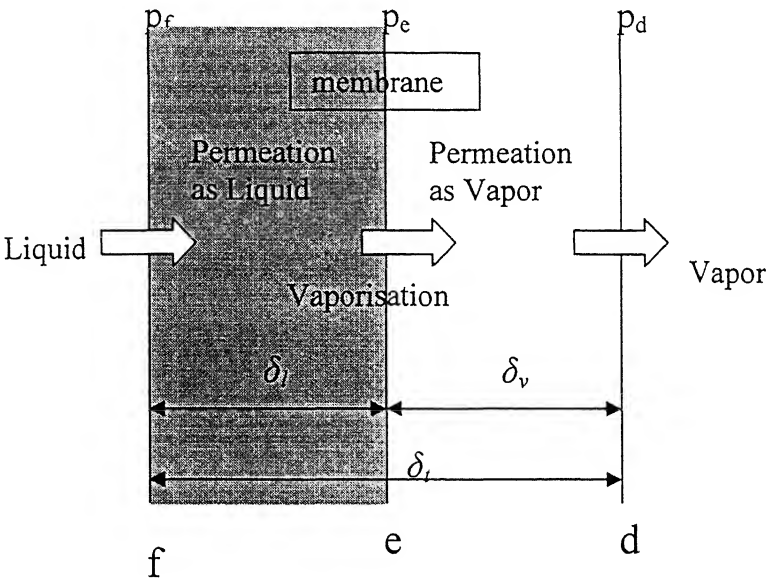

Figure 2.4 Schematic description of pseudophase change solution-diffusion (PPCSD) model

Although numerous models based on these above mentioned postulates have been proposed, many of them are solely based on qualitative observations and vigorous verification by experimental data is lacking. Each model works for some systems, but none is general enough to make good descriptions and predictions for most systems.

2.6 Pressure Profile and Location of Vaporization

In solution-diffusion the fluids on both sides of the membrane are considered to be in equilibrium with their respective membrane interfaces. It is not explained where the phase change occurs. Also it assumes constant pressure inside the membrane. The apparent indifference to address the problem of phase change in the model is the main

challenge to the model. It is interesting to note here that pervaporation was named so, due to its hybrid nature, i.e., the presence of liquid and vapor phases.

Pore flow model was first of its kind to answer the location of vaporization in a pervaporation process. It assumes a pressure drop from feed side pressure to saturation vapor pressure at the location of vaporization, which is the driving force for liquid flow. And as soon as it changes the phase, it will diffuse through the pores obeying a suitable mechanism according to the pore size and its distribution and the pressure. The flux is proportional to the square of pressure. Pressure drop in the vapor permeation zone is from saturation vapor pressure to applied downstream pressure.

The pseudophase change solution diffusion model was an attempt in the same direction of pore flow model. The length of the permeation zone that behaves as a liquid permeation mechanism as well as the pressure and concentration profile within the membrane were calculated. The location of vaporization was determined on the basis of saturation vapor pressure of the permeating component. The pressure profile within the membrane system was also investigated. The pressure drop is linear and abrupt, from feed side pressure to saturation vapor pressure in the zone that behaves as a liquid permeation process, while in the zone that behaves as a vapor permeation process, the pressure decreases slowly to applied downstream pressure. Concentration of permeant in the liquid zone is considered to be a constant in this model, while it decreases gradually and drops to zero as the interface of the permeate side and membrane system is approached at zero downstream pressure.

Chapter 3

Theoretical

3.1 Pervaporation –Process definition

This is a passive process and the driving force for molecular or particle transport s the chemical potential difference. The feed liquid mixture which is to be separated is placed in contact with one side of the membrane. The liquid permeates through the nembrane and the permeating liquid is removed as vapour from the downstream side. Phase change occurs by keeping downstream pressure lower than the saturation pressure of the permeating component. Such conditions can be maintained through the application of a vacuum pump or sweeping gas (normally air or steam) on the downstream side. The permeate vapour is condensed and collected or released as desired. Application of vacuum thus requires very low temperature condensation of permeating components; usually through the use of liquid nitrogen. It is assumed that the membrane acts as a thin solvent layer and the pervaporate composition is mainly governed by preferential solvation of the polymeric barrier material. As a result, the liquid – vapor equilibrium is greatly perturbed. Permeating components get vaporized by taking latent heat from feed iquid. Therefore, external heating is required to make up the loss of enthalpy and to naintain the isothermal conditions. A schematic diagram of the process is shown in igure 3.1.

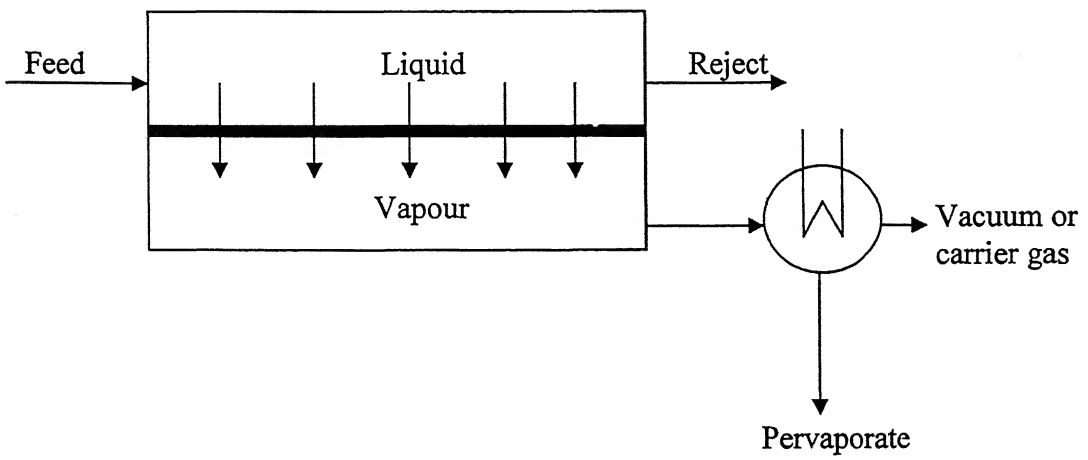

2 Chemical Potential and Activity

The most important partial molar quantity concerned in chemical thermodynamics the partial molar free energy, a quantity known as the chemical potential. It is defined r a specified state of aggregation, a specified temperature, and an arbitrarily chosen but specified standard pressure [37]. One can use changes in chemical potentials to lculate changes not only in free energy but also in work content, energy, enthalpy and ıtropy depending upon the constraints imposed on the processes; thus, demonstrating its ıiversality. Just like other membrane separation processes, in pervaporation also, the vo sides of the membrane are subjected to two different environments so that a chemical ɔtential difference exists across the thickness of the membrane. Permeating liquid passes ırough the membrane from high chemical potential side to low chemical potential side.

The activity, a_i of a component '*i*', in a liquid or solid mixture is a quantity of unit imension, defined in terms of the chemical potential μ_i:

$$\mu_i = f_i(T) + RT \ln a_i \tag{3.1}$$

here, $f_i(T)$ is a function of temperature, T only; and it is called *standard chemical otential*, μ_i^o. So, Eq. 3.2 is written as:

$$\mu_i = \mu_i^o + RT \ln a_i \tag{3.2}$$

he ratio of activities of a substance in two different states and at the same temperature ill depend only on the difference in chemical potential. Before a numerical value can be ssigned to activity, some kind of reference function must be assumed and some articular state must also be chosen in which the activity approaches or equals the value f the reference function. If $g(\zeta)$ is a reference function in which ζ is a parameter for any f the variables like concentration, pressure, mole fraction or some other similar variable hat might be used in conjunction with temperature for describing the system. We can hen define generalized activity as,

$$\lim_{\zeta \to \zeta^*} \frac{a_i}{g(\zeta)} = 1 \tag{3.3}$$

Here, ζ^* is the value of ζ in the reference state (activity equals the value of the reference unction). As an example, consider a binary system for which x_i is the mole fraction of

one of the components. Then, we say that the activity approaches the mole fraction as the solution becomes infinitely dilute,

$$\lim_{x_i \to 1} \frac{a_i}{x_i} = 1 \tag{3.4}$$

Here, the pure liquid is the reference state and the activity of the pure liquid is equal to unity. Fugacity is a special kind of activity, defined for conveniently dealing with the gases. It has all the attributes of activity; specifically, it involves the pressure as the reference function and zero pressure as the reference state. Fugacity concept can be extended to liquids and solids (as well) by simply assigning to a liquid (or solid) a fugacity numerically equal to that of vapour in equilibrium with it. Obviously, a ratio between fugacity for any two states at the same temperature must be identical with the ratio of activities associated with the same two states regardless of the functionality of the activity. Hence, if we know the fugacity of a component in each of two states, we can determine a ratio of activities for those two states. It one of those states is the reference state for activity, we can evidently determine the activity for the other state. A similar argument can be applied to switching from one activity representation to another without recourse to fugacity.

3.3 Mass Transport within the Membrane and Membrane selection

The main criteria for assessing the usefulness of a membrane are the selectivity and the permeation flux. In pervaporation, the flux is usually quoted as mass flux, J in $kg.m^{-2}.h^{-1}$. In practice, one can expect to obtain a higher value of J in pervaporation mode than in reverse osmosis mode for the same membrane [38, 39].

One measure of selectivity is the separation factor defined as:

$$\alpha_{AB} = \frac{w_A^{''} / w_B^{''}}{w_A^{'} / w_B^{'}} \tag{3.5}$$

where, $w_A^{'}$, $w_B^{'}$, $w_A^{''}$ and $w_B^{''}$ denote the weight fractions of component A and B in the feed solution and in the pervaporate, respectively. The subscript A is the species that is preferentially pervaporated. A more convenient expression for the selectivity is given by enrichment factor β:

$$\beta = \frac{w_A''}{w_A'} \tag{3.6}$$

The fractionation efficiency of a polymer film can be increased by inserting an agent used in extractive – distillation or solvent – extraction process. For example, a viny-li-dene fluoride film plasticized with 3-methyl-sulpholene was found to be an effective permselective membrane for the extraction of benzene from cyclo-hexane. The addition of 17% 3-methyl-sulpholene results 15 % increase in the flux; while the enrichment factor β decreased slightly from 1.9 to 1.8 [40]. In this regard, Larchet and Brun inserted nitrile functional group into poly-butadiene by copolymerization with acrylo-nitrile. Another promising modification of membrane is to include Werner [41] complexes so as to mimic clathration processes.

Cabasso and Mulder [42] used Hansen's [43] three-dimensional solubility parameter to predict the separation capabilities of polymeric membranes toward liquid mixtures. Hansen [43] suggested representing every organic compound by three dimensional coordinates (δ_d, δ_p and δ_h) which reflect London forces in terms of polar forces and hydrogen bonds, respectively. Similarly, every polymer can be represented by volume bounded by coordinates by all those compounds that acts as solvents for the polymer. Thus, organic compounds whose coordinates are not within the boundaries of a polymer solubility volume are not solvents for polymer.

For the separation of a given mixture *A-B*, Cabasso [42] suggested selecting a polymer soluble in *A* and insoluble in *B*. The selectivity is expected to be highest when *A* is closest to the centre of solubility area and *B* is located far from the solubility boundary. To prevent the dissolution of such a membrane, the active polymer can be alloyed with another polymer or grafted onto such a polymer. Figure 3.2 shows the solubility areas for an alloy-membrane composed of cellulose acetate and poly-phosphonate. This membrane is very efficient in separating an azeotropic mixture such as benzene-cyclohexane (α=16) or ethanol-heptane (α=10.3). The separation factor is significantly smaller for the mixture styrene - ethylbenzene (α=1.3) because of the solubility area of the poly-phosphonate falling within the respective two components.

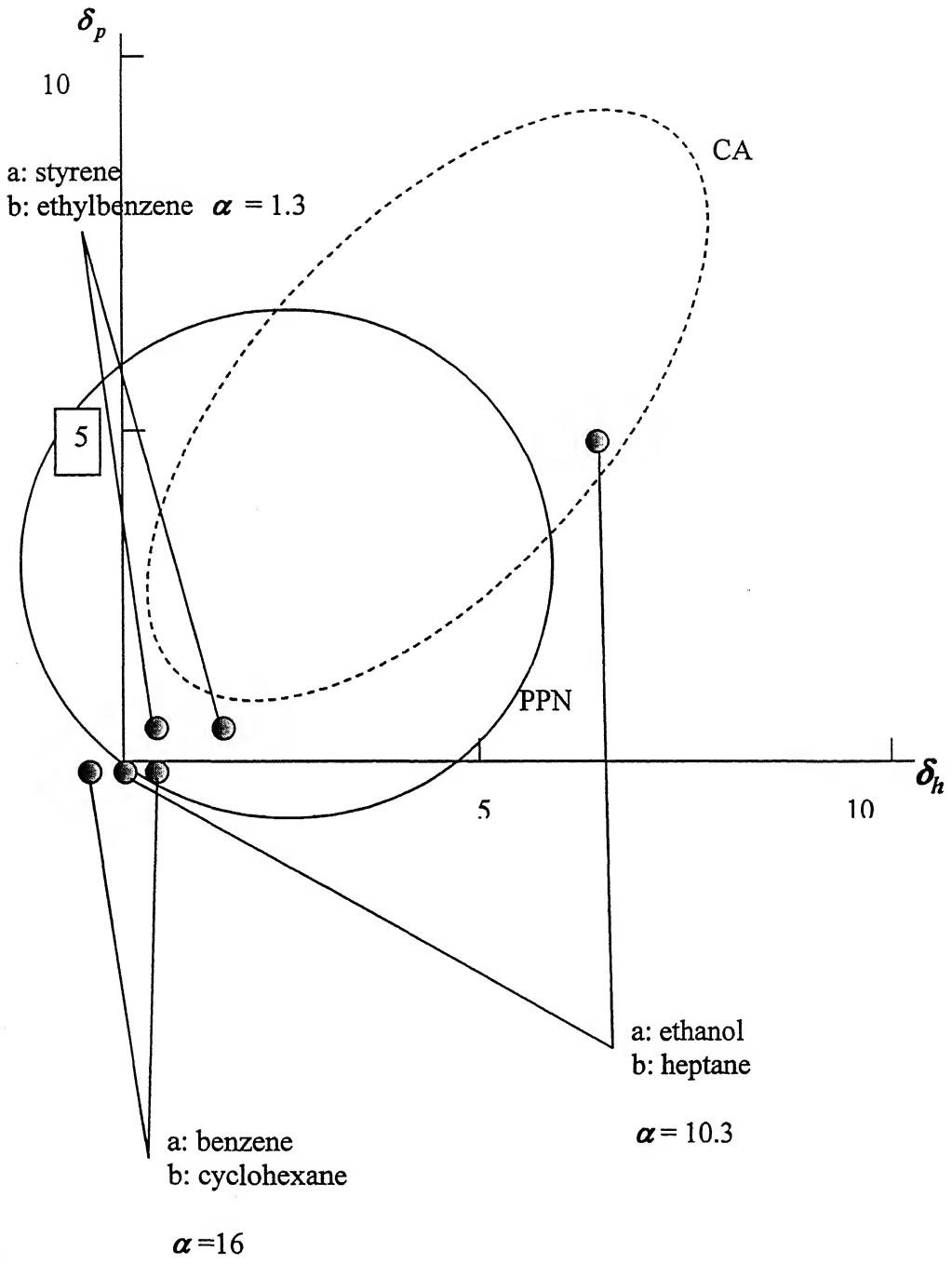

Figure 3.2: Solubility parameter diagram of PPN/CA alloy membrane
α - Separation Factor for the azeotropic composition
PPN: Poly-phosphonate CA: Cellulose acetate

3.4 Characterization Methods

3.4.1 Contact Angle

The angle formed at a point on the line of contact of three phases, of which at least two are condensed phases, by the tangents to the curves obtained by intersecting a plane perpendicular to the line of contact with each of three phases. One of the phases must be a liquid, another phase may be solid or liquid and the third phase may be gas or liquid. Experimentally, when a liquid is contacted with a solid and another phase, it is usually observed that the contact angle does not reach its equilibrium value instantaneously. It reaches a mechanical equilibrium after some time. A schematic diagram when contact angle reaches equilibrium is shown in Figure 3.3.

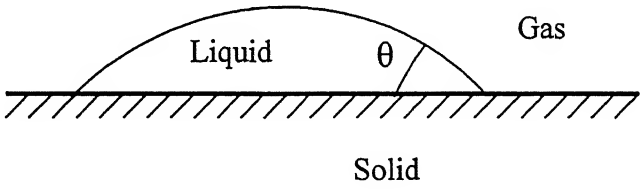

Figure 3.3: Contact Angle θ, made by a liquid on a solid surface

A simple, but very useful relation, known as Young-Dupré equation, can be derived for this situation:

$$\gamma_i \cos\theta = \gamma_m - \gamma_{mi} \tag{3.7}$$

where, θ is the contact angle made by the liquid i, on the solid m. γ_i and γ_m are the surface tensions of liquid and solid, respectively; γ_{mi} is the interfacial tension between them. This equation regards the respective surface tensions as virtual or actual forces parallel to the surfaces. If the contact angle is greater than 90°, the liquid is considered not to wet the solid and in other words liquid will not tend to enter the capillaries of the solid. The smaller the contact angle between the liquid and the solid, spreading of liquid over solid surface is more even or the liquid may adhere to the solid surface until $\theta \approx 0°$. At this point complete wetting of the solid takes place. The situation of complete wetting is best illustrated in terms of spreading coefficient, defined as:

$$S_{im} = \gamma_m - \gamma_i - \gamma_{mi} \quad (3.8)$$

ıere, S_{im} is the spreading coefficient of *i*, on *m*. Generally spreading occurs when a ıuid of low surface tension is placed on a solid of high surface tension. Positive reading coefficient means spontaneous spreading accompanied by a decrease in free ergy. Actually, spreading coefficient is the difference between work of adhesion of *i* to and work of cohesion of *m*.

ł.2 X-Ray Diffraction (XRD)

X-rays are electromagnetic radiation with typical photon energies in the range of 0 eV - 100 keV. For diffraction applications, only short wavelength x-rays (hard x-/s) in the range of a few angstroms (around 0.1 angstrom at 1 keV - 120 keV) are used. rays are produced generally by either x-ray tubes or synchrotron radiation. X-rays marily interact with electrons in atoms. When x-ray photons collide with electrons, ne photons from the incident beam will be deflected away from the direction where :y original travel; much like billiard balls bouncing off one another. If the wavelength these scattered x-rays did not change (meaning that x-ray photons did not lose any :rgy) the process is called elastic scattering or Thompson Scattering; where, only ımentum has been transferred in the scattering process. The peaks in the x-ray fraction pattern are directly related to the atomic distances. For a given set of lattice ne with an inter-plane distance of *d*, the condition for a diffraction (peak) to occur can simply written as $2dSin\theta = \lambda$ (known as Bragg's Law).

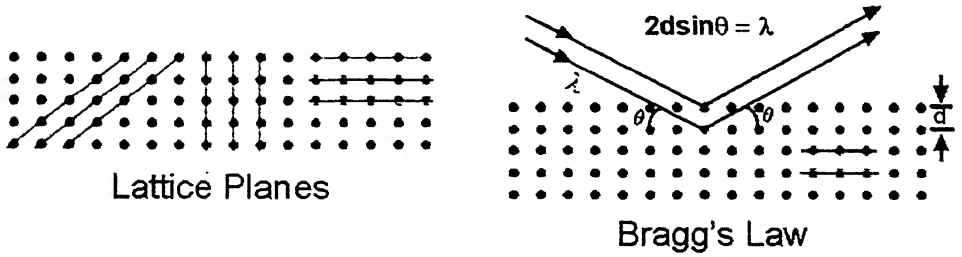

Figure 3.4 Typical diffraction pattern in lattice planes, Bragg's law

Many types of X-Ray diffraction technique are available such as power diffraction, thin film diffraction, small angle X-ray scattering (SAXS), wide angle X-Ray scattering (WAXRD). In this study we are using WAXRD as it is widely used for determining polymer structure.

3.4.3 Fourier transform infrared spectroscopy

Fourier Transform Infrared Spectroscopy (FTIR) is an analytical technique used to identify organic (and in some cases inorganic) materials. This technique measures the absorption of various infrared light wavelengths by the materials of interest. These infrared absorption bands identify specific molecular components and structures. Absorption bands in the range of 4000-1500 wave numbers are typically due to functional groups (e.g. -OH, C=O, N-H, CH3, etc.). The region between 1500-400 wave numbers is referred to as the finger-print region. Absorption bands in this region are generally due to intra-molecular phenomena and are highly specific for each material

Material Identification - The unknown IR absorption spectrum is compared with standard spectra in computer databases or a spectrum obtained from a know material to determine the identity of the material being analyzed. In this regard, one can also use FTIR for identifying foreign materials such as particulates, fibers, residues, etc.

Quantification - Quantitative concentration of a compound can be determined from the area under the curve in characteristic regions of the IR spectrum. Concentration calibration is obtained by establishing a standard curve from spectra for samples of known concentrations.

3.4.4 Positron annihilation lifetime spectroscopy (PAL)

Positron annihilation technique [44] has developed into a powerful characterization tool for the study of free volume sizes and free volume fraction in polymeric materials. By measuring the lifetimes of the positrons, one can get fairly accurate estimates of the free volume in angstrom (2-10 Å) range. Contrary to other methods, PAS is capable of determining the holes and free volume in a polymer without being significantly interfered by the bulk. When positrons are implanted into a polymeric

material, some of them interact with the electron clouds in the material to annihilate and give two gamma rays of energy 511 keV each. However, a fraction of positrons combine with the electrons to form a hydrogen-like quasi-stable atom, known as positronium and denoted as Ps. Depending upon the spin alignment, positronium could be in the form of para-positronium (p-Ps) or ortho-positronium (o-Ps). The positronium atom preferentially gets localized within the free volume cavities and annihilate after an average time characteristic of the shape and size of the free volume. Positron annihilation lifetime spectra are analyzed in terms of three lifetime components, viz: para-positronium (p-Ps) annihilation, τ_1; free positron and positron-molecular species annihilation, τ_2; and o-Ps annihilation, τ_3. While τ_1 and τ_2 are of the order of few hundred picoseconds, τ_3 is of the order of nanoseconds. Each lifetime has an intensity I, corresponding to the fraction of annihilations taking place with the respective lifetimes. The parameters τ_3, I_3 corresponding to the decay of o-Ps provide the size-specific information for free volumes and pores.

Free volume radius r is obtained by first considering o-Ps trapped into a spherical volume with radius r_0, providing infinite potential barrier. The Schrödinger equation is solved to obtain the positronium wave function for the centre of mass motion of o-Ps in the ground state. The o-Ps pick-off annihilation rate is then calculated through a semi-empirical approach, by assuming a homogeneous electron layer with a thickness of Δr (= $r_0 - r$ = 0.166 nm) adjacent to the wall and calculating the overlap of positronium wave function with the electron layer. Accordingly, the following expression may be obtained, which relates o-Ps pick-off lifetime, τ_3 and free volume radius [45-47].

$$\tau_3 = \frac{1}{2}\left[1 - r/(r+\Delta r) + \left(\frac{1}{2\pi}\right)\sin\left(\frac{2\pi r}{r+\Delta r}\right)\right]^{-1} \tag{3.9}$$

Further, the fractional free volume f may be estimated from the following empirical relation.

$$f = CV_F I_3 \tag{3.10}$$

Where V_F is free volume and the scaling factor, C, is obtained from variation of free volume with temperature. However, in the absence of such data, it may be typically assigned a value of 1.0 [48]. Equation (3.9) can also be used for cylindrical free volume

pore) with the value of Δr set at 0.196 nm [49]. In this case, for the same lifetime value, one gets a higher value for the radius as compared to the spherical case.

Chapter 4

Experimental

4.1 Materials and Chemicals

a) Toluene (99.5 wt%) from Ranabaxy ,India
b) Acetone (99 wt%) from Qualigens , India
c) Ethyl cellulose (ethoxy content 48 -49.5% from Loba–Chemie , India)
d) Hydrazine hydrate(64 wt%) from Qualigens , India
e) 2056 Polystyrene from Otto Kemi, India
f) Poly-acrylonitrile-co-butadiene-co-styrene: *CAS no 43,013-7* from Aldrich chemical company, Inc.
g) Sulphuric acid (98 wt%) from S-D fine chemicals Ltd, India
h) Benzene (99.7 wt%) from Ranabaxy, India
i) Cellulose acetate from S-D fine chemicals Ltd, India
j) Liquid Nitrogen, supplied from liquid nitrogen plant, I.I.T Kanpur

4.2 Instruments and other auxiliary accessories:

a) Membrane casting unit

I. Thin film applicator (ACME), India
II. Automatic film applicator from BYK Gardener, Germany

b) Cell

The pervaporation test cell is made of glass consisting of a pair of "cups" kept face to face so that the membrane can be secured in between with the help of specially designed flanges (Figure 4.1). One such "cup" has an approximate diameter of 90 mm and a length of 100 mm to provide an approximate volume of 400 ml. It provides an effective membrane area of 50.4 cm^2.

c) Peristaltic Pump

I. Model – Miclins, VSP 100, Rollers – 4, Tube size supported – 4mm to 8mm bore size wall thickness 1.5 mm
II. Flow rate – 0.15 L/min -1.5 L/min (+/- 3% accuracy) and Max. Speed – 1500 rpm (Forward/Reverse)

d) Vacuum Pump

I. Type – Double stage Rotary vacuum pump VT 2012, Motor – 0.5 H.P., Vacuum Techniques Pvt. Ltd., Bangalore, Oil Charge – 0.75,

II. Pumping speed -- 250 L/min, R.P.M. – 1440

e) Pirani Guage

Model: VT-DHP-11, Vacuum Techniques Pvt. Ltd., Bangalore

f) PID - Controller

I. Model – 1) TIC-03, Blue Bell 2) PG16, Fuji, Japan

II. Range – 0-200 ^{0}C and accuracy - ± 0.1 ^{0}C

g) Weighing Balance

Afcoset electronic balance, Accuracy – 0.0001 g

h) Gas Chromatograph

I. Nucon-5700

II. Data station and software - (AIMIL, Delhi)

III. TCD, Thermal Conductivity Detector with Column - Chromosorb 103

IV. Column specification :

Length: 6 ft *od*: 1/8 inch *id*: 2 mm *Mesh range*: 60 -80 *Maximum (Permissible) Temperature of the Column*: 250 °C

4.3 Preparation of membrane

4.3.1 Polymer solution

Ethyl cellulose (EC) polymer (15 g) was dissolved in toluene (85 g). The solution was centrifuged (REMI model -R 24, India) at 10,000 rpm for 15 minutes for the removal of un-dissolved polymer. The supernatant homogeneous solution was transferred to a conical flask (air tight) and kept for overnight for the removal of entrapped air bubbles. Similar procedures were followed for preparing polymer solution with acrylonitrile styrene butadiene (ABS-15 wt %) and polystyrene (PS-15 wt %).

4.3.2 Blending

Ethyl cellulose polymer and ABS polymer was mixed on a definite weight ratio. The prepared solution was continuously stirred at around 3000 rpm (REMI

5MLH, India) for 1 day. The solution then became homogeneous. It was further kept for 1 day for removal of any traces of entrapped air bubbles.

4.3.3 Casting

The casting of membrane was carried out on a glass plate using a modified thin film applicator (ACME, India) as well as automatic film applicator (BYK Gardener). After around 24 hours of solvent evaporation, the membrane was placed in vacuum oven for another 4 hours for the removal of residual traces of solvent. Similar procedures were followed for casting polystyrene (PS) based membranes. Varying proportions of blended membranes (ABS & EC polymers) are given new names and are reported in Table 4.1.

Quantity (in g) of EC : ABS in 100g of polymer solution	*100:0*	*80:20*	*70:30*	*60:40*	*30:70*	*20:80*	*0:100*
Membrane	EC	BABS1	BABS2	BABS3	BABS4	BABS5	ABS

Table 4.1: Composition along with notations of blended membranes

4.3.4 Modification of polymer

Around 400 ml of 98% sulphuric acid or appropriately diluted sulphuric acid was taken in a 1000ml beaker. Further, the casted PS membrane was dipped carefully in the solution. The reaction mixture was kept for 1 hr for complete sulphonation to occur. After 1 hr, water was added to decrease the concentration of sulphuric acid. Further, the membrane was slowly taken out from reaction mixture to avoid any structural damage in the membrane. The membrane was then kept for drying in atmosphere. Introduction of sulphonic acid group was ascertained through FTIR spectrum of the polymer. The reaction between polystyrene and sulphuric acid in room temperature may produce sulphonated polystyrene, according to reaction shown in Fig. 4.1 [50].

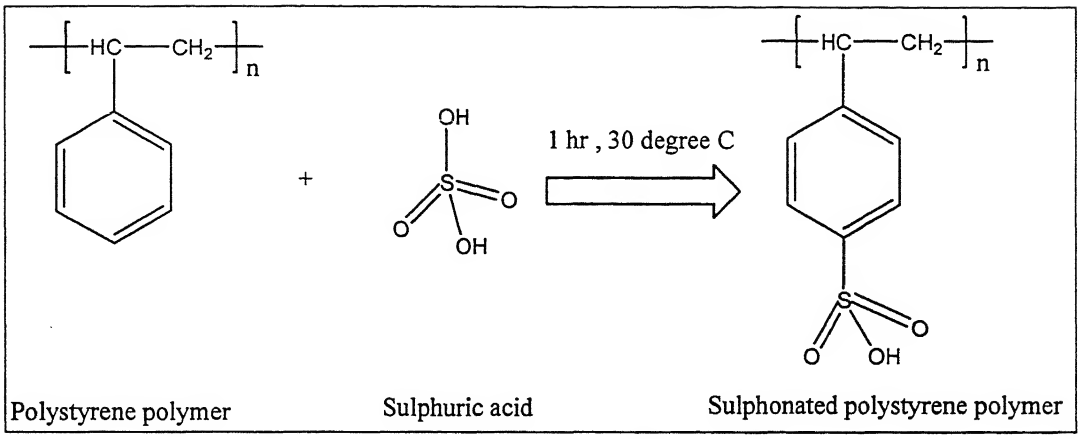

Figure 4.1- Reaction between Polystyrene and Sulphuric acid

The notations of modified PS (MPS) membranes with respect to reactions with varying concentration of sulphuric acid are reported in Table 4.2.

Concentration of sulphuric acid (wt %)	*50*	*60*	*70*	*80*	*98*
Membrane	MPS0	MPS1	MPS2	MPS3	MPS4

Table 4.2: Composition along with notations of modified PS membranes

4.4 Membrane density: Measurements

Approximately 30 x 30 mm membrane piece was cut. The thickness of these membranes was then measured using vernier calipers. Further, these membranes were weighed using weighing machine mentioned above. Thus the membrane density was measured using equation: $\rho = m/v$ (4.1)

where, m and v are mass and volume of the membrane respectively. The values of length, width and thickness are given in Appendix C.1.

4.5 Contact Angle: Measurements

Equilibrium contact angles of water and hydrazine hydrate with membranes were measured in saturated environment through sessile drop method using Goniometer (Rame-Hart, inc. Imaging System, USA). Flat sheets were mounted using stainless steel holder and placed in environmental chamber. A glass syringe with a stainless steel needle was used to put the liquid drop on membrane. The angles were measured with RHI software by capturing the image with video camera. Around 5 minutes stabilization time was allowed to capture the image. Around 50 readings were then recorded in a time span of 1 second and from the average of these readings, an estimation of angle was made. Further, four or five such measurements were made for each liquid on the same membrane and the average value was noted.

4.6 Sorption

Pre-weighed dry membranes were taken in a conical flask containing water or hydrazine hydrate for sorption purpose. The flask was kept on shaker bath (model SW-23, Julabo, Germany) under 200 rpm for 6-7 days at 50°C. The membranes in conical flasks were taken out at regular intervals and were wiped with tissue paper for the removal of adhered liquid. The wet weight of the membrane was measured. The procedure was repeated until consecutive readings of weight of wet membranes were found equal. The difference of weights was presented with respect to dry weight of membranes as percentage of sorption.

4.7 Analysis

Hydrazine is a hygroscopic substance which is prone to air oxidation. Further, under exposure to atmosphere it absorbs carbon dioxide and, therefore, analysis of hydrazine sample requires proper precautions. The tedious procedure involved in *Penneman method* [51] of employing potassium iodate as titrant i.e. prone to errors. Therefore, gas chromatograph method [52] was employed for analysis of hydrazine. Concentrations in both the feed and the permeate samples were measured. Gas chromatograph (Nucon, India equipped with TCD) with *Puropack-Q* as reference column and chromosorb-103 as main column was employed for the purpose. The injector, detector and oven temperatures were set at 210, 220 and 170°C, respectively.

Helium was used as a carrier gas at 20ml/min. Observed retention time for water was 1.0 and that for hydrazine was 2.46 minute for above stated conditions.

4.8 Pervaporation: Set up and Procedure

A set-up was designed and developed for the pervaporation experimental investigations and a schematic version is shown in Figure 4.2. Pervaporation test cell, made of glass, was having specially designed flanges to lodge the membrane with an effective membrane area of 50.4 cm^2. Membrane was first cut into circular shape (90 mm diameter). The membrane was then kept on a highly porous stainless steel support with the shiny dense polymeric layer facing the feed solution. Initially fixed volume of feed solution (hydrazine hydrate of 64 wt% of hydrazine) was taken on the upper side (feed side) of the cell. Both upstream and downstream sides of the cell were heated (in order to maintain isothermal conditions around the cell [53]) and hence cell surface was covered by heating mantels. The temperatures of both the sides were controlled at 50°C, using PID controller device (Fuji, Japan).

The membrane upstream side was kept at atmospheric pressure and the downstream side was maintained under vacuum, using a vacuum pump (Vacuum Techniques, Bangalore). The condenser system consisted of two traps that can be used alternately, allowing the permeated pervaporate stream to be sampled continuously without interruption of the operation. The permeated vapors are condensed in the trap, which is kept in Dewar flask, filled with liquid nitrogen. The frozen permeate was collected within a specified time interval. The cold traps were brought to room temperature for measuring its weight, using a five decimal balance, to determine mass flux. Permeate was analyzed to determine its hydrazine content. Flux values and hydrazine concentration in permeate were recorded as a function of time. The values of flux and selectivity's are shown in Appendix B.1 to B.13. To minimize the measurement error, an average of two separate consecutive readings were taken after the system reached to steady state. Thus, for analysis all steady state values of flux and selectivity's were used.

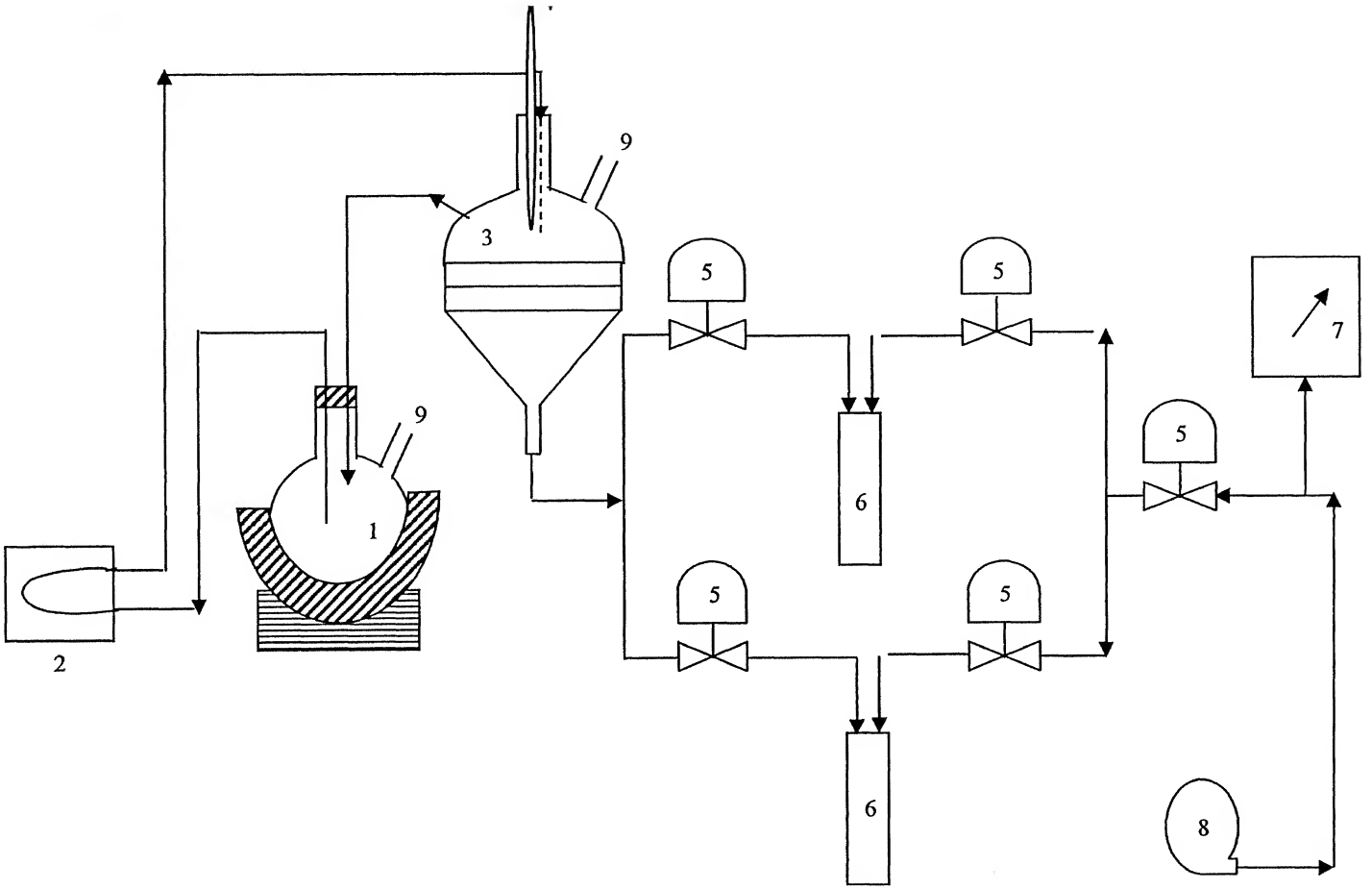

1—Preheating Cell, 2—Peristaltic pump, 3—Pervaporation cell, 4—thermocouple, 5—Needle valves, 6—Liquid traps placed in Dewar flask, 7—McLeod Gauge, Pirani gauge, Capillary column in parallel mode 8—Vacuum Pump, 9—Condenser

Figure 4.2: Schematic diagram of the experimental setup for pervaporation

Chapter 5
Results and Discussions

The selection of polymer for hydrazine separation plays an important role due to high alkaline nature of hydrazine (pH>12.5) and only few polymers are available that may withstand such high alkalinity. Further, hydrazine has strong reducing and hydrolyzing effects. Ravindra et al have used ethyl cellulose (EC) membrane to carry out this separation. Even though, ethyl cellulose is highly selective for water at low concentrations of hydrazine, it, however, gives low selectivity for 64% aqueous hydrazine solution. Further, it was reported that ethyl cellulose is selective for hydrazine during sorption and selective for water during diffusion.

Therefore, such a problem may be addressed by selecting a membrane with high water-perm selectivity. This may be achieved by increasing the sorption selectivity (water to hydrazine) or diffusion selectivity. Various hydrophilic chitoson and modified chitoson membranes were previously used and were found to have low selectivity's. Again for better diffusion ratio, the hydrophobic moiety may be introduced into the polymer chain. This may, however, decrease permeation rate. Thus, with the introduction of balanced quantities of hydrophilic and hydrophobic moieties better flux and better selectivity may be obtained. In this regard, one may combine the properties of hydrophilic and hydrophobic polymers while casting a membrane and may thus achieve high values of flux and selectivity.

The present work, therefore, contemplates to combine (by blending) the hydrophilic and hydrophobic properties of ethyl cellulose and ABS polymers, respectively. This was attempted by blending both of these polymers in solution state and in different proportions. The procedure for such blending is described in the previous section 4.3.2. Following paragraphs, therefore, present and discuss the salient results of PV studies of hydrazine hydrate from such polymers (in the form of membranes - obtained in different values of thickness).

5.1 Separation study of blended ABS & EC membranes

In the PV process, the feed mixture is contacted with a non-porous perm selective membrane and separation can be explained by the solution-diffusion mechanism which involves steps of sorption (into), diffusion (through) and desorption (from) [54]. The first and the last steps are usually considered to be fast and to take place at equilibrium; whereas, diffusion is a slower process.

The effects of blending on permeation rate and product concentration were studied by keeping other parameters constant (temperature: 50°C, downstream pressure: 0.1mmHg, static feed condition). The permeate flux ($kg/m^2.h$) was calculated using equation 5.1

$$J = \frac{A}{m \times t} \tag{5.1}$$

where, J is the permeate flux, m is the weight of the permeate, A is the membrane area and t the time of operation. Membranes were produced of varying thickness; therefore, the flux was normalized to a membrane thickness of 5 μ m and denoted as $(J)_I$ using equation 5.2.

$$(J)_I = \frac{J \times l}{5} \tag{5.2}$$

where, l is the membrane thickness. Such normalization was based on Fickian behavior during mass transport through the membrane.

Further, flux is inversely proportional to both membrane density and thickness. Thus another method for normalizing flux may be the product of flux, membrane density and membrane thickness. Therefore, the second type of normalize flux denoted as $(J)_{II}$ was derived using the following equation (5.3).

$$(J)_{II} = J \times \rho \times l \tag{5.3}$$

The values of flux, normalized flux, polymer density and thickness are tabulated in Table 5.1. Further, the flux and $(J)_I$ & $(J)_{II}$ values for different blended and pure polymeric membrane (EC+ ABS) are also plotted in Fig. 5.1to 5.3.

5.1.1 Influence of ABS composition in blended membrane on Flux

Fig. 5.1 describes the experimental values of flux observed with different membranes (EC, BABS1 to 5, ABS). It may be observed from Fig. 5.1 that the values (in the form of bars) do not show any trend with continuous addition of ABS in EC to produce different membranes. As mentioned earlier, this may be due to varying thickness of membranes (also inscribed on respective bars on membranes). Thus, the values of flux were normalized by using equation 5.2. Accordingly, the calculated values of $(J)_I$ was plotted (Fig. 5.2) with varying composition of ABS. As expected, the Fig. 5.2 gives a trend which is in the form of sigmoidal decay. Obviously, such a trend visualizes an initial slow decline with significant decline at later stages. Therefore, between BABS3 to BABS4 & 5, there is significant decline of flux with higher dosage of ABS in EC polymer.

Although a trend was observed in Fig. 5.2 but it was felt that density of the blended polymer may play an important role in normalizing flux. Accordingly, another form of normalized flux was defined (as per equation 5.3). Normalized flux $(J)_{II}$ was plotted in Fig. 5.3 against composition of ABS in blended membrane. Interestingly, a linear relationship was observed.

The polymer ABS is a mixture of three polymers; namely acrylonitrile, butadiene and styrene. Butadiene and styrene are hydrophobic in nature whereas acrylonitrile has hydrophilic property. Thus, the compound ABS has both hydrophilic as well as hydrophobic characteristics; though the hydrophobic part is generally dominant. EC is a strong hydrophilic polymer. As we move from left to right in Fig. 5.1, the quantity of ABS in the blended polymer increases. From the graph it is clear that apart from BABS1 the flux decreases as the ABS quantity in the blended membrane (BABS-1 to 5) increases. This is due to increase in hydrophobic (ABS) character. Similar attributions were made in an earlier work on hydrazine hydrate system by Satyanarayana and Bhattacharya [10].

Further, from the Fig. 5.3 we can estimate a relationship between $(J)_{II}$ and composition of ABS. We find a linear relationship with a correlation coefficient of 0.995 and it is denoted in Eq. 5.4

$$(J)_{II} = 9.4436 - 0.0986\ (ABS) \qquad (5.4)$$

where, ABS is in wt % in the blended membrane. This may prove useful to estimate normalization flux, $(J)_{II}$ for blended polymers of unknown composition of ABS.

Membrane	*Thickness, l (m) x10^6*	*Polymer density, ρ (kg/m^3)*	*Flux, J (kg/m^2.h) x10^3*	*Normalized Flux, $(J)_I$ (kg/m^2.h) x10^2*	*Normalized Flux, $(J)_{II}$ (kg^2/m^4.h)x10^4*
EC	60	1004.82	8.042	9.650	4.11
BABS1	80	941.18	9.571	15.313	7.21
BABS2	40	1017.18	16.928	13.542	6.89
BABS3	70	778.36	9.956	13.938	5.42
BABS4	110	1116.67	1.967	4.326	2.42
BABS5	60	1189.32	2.274	2.728	1.62
ABS	75	950.41	5.763	8.645	4.85

Table 5.1 –Experimental and normalized values of flux obtained for blended membranes along with the properties

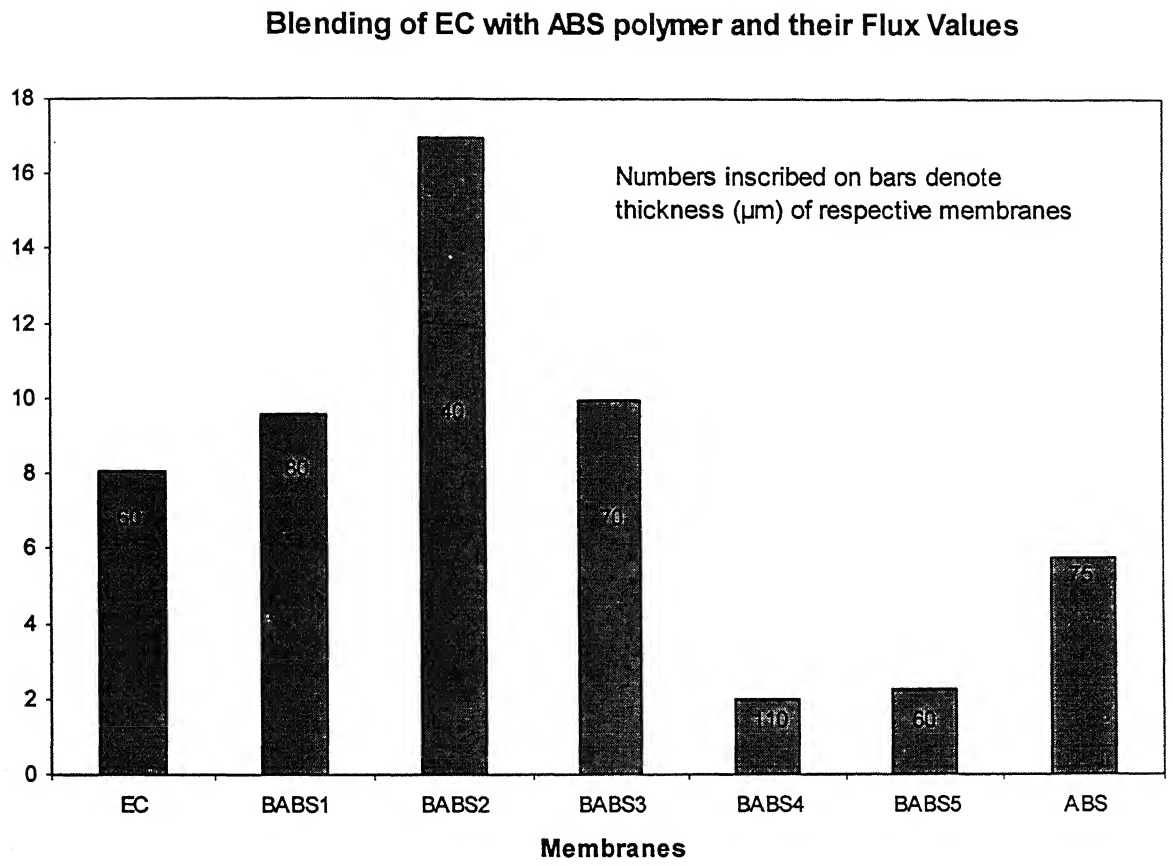

Figure 5.1 – Flux values for different blended membranes

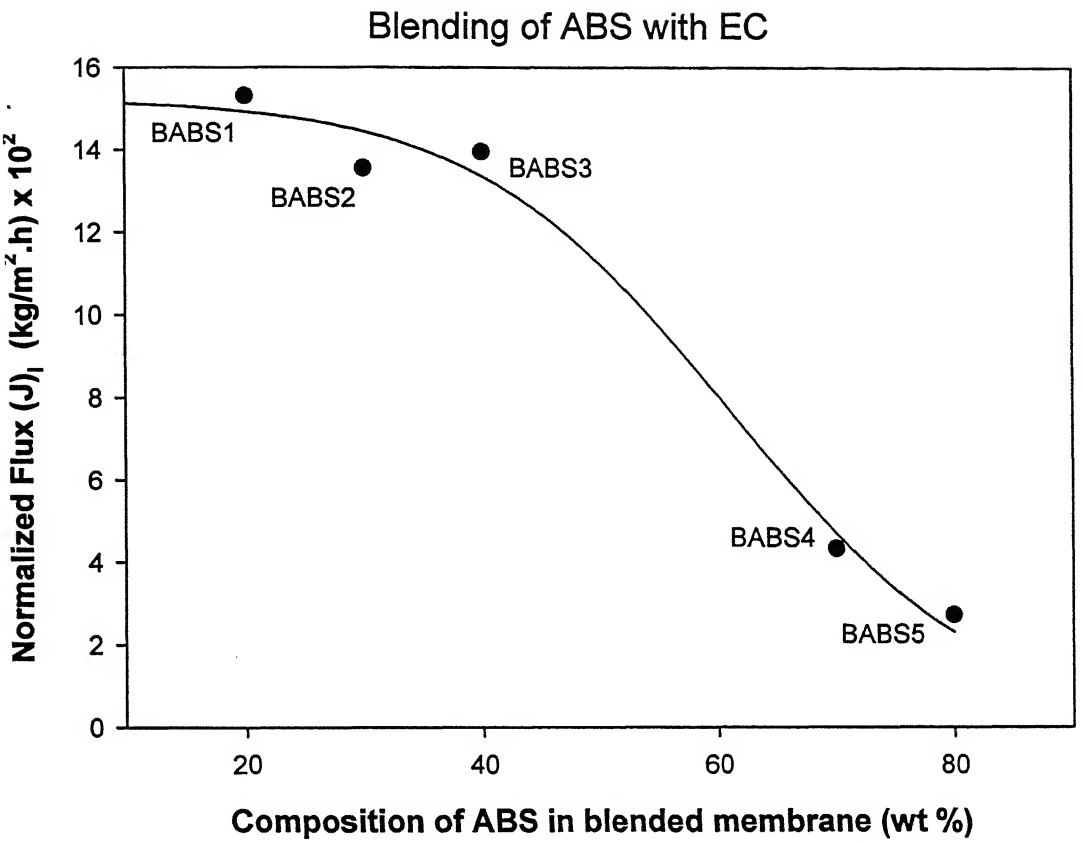

Figure 5.2 – Normalized Flux $(J)_I$ variation with varying composition of ABS polymer in EC polymer for blended membranes

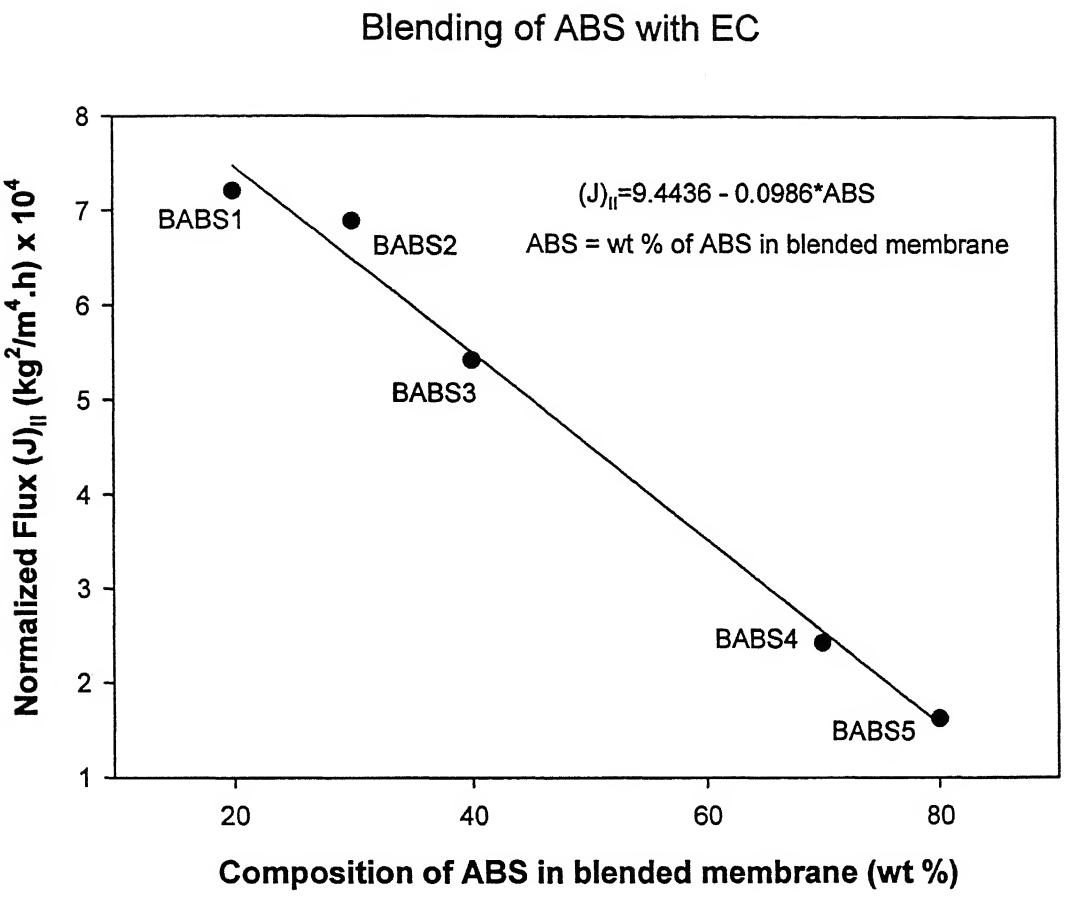

Figure 5.3 – Normalized Flux $(J)_{II}$ variation with varying composition of ABS polymer in EC polymer for blended membranes

5.1.2 Influence of ABS composition (on membrane) on Selectivity and PSI index

The measure of selectivity in the pervaporation experiments is the separation factor defined as:

$$\alpha_{AB} = \frac{w_A^{''} / w_B^{''}}{w_A^{'} / w_B^{'}} \tag{5.5}$$

where, $w_A^{'}, w_B^{'}, w_A^{''}, w_B^{''}$ denotes the weight fractions of component A and B in the feed solution and in the pervaporate respectively. The subscript A is the species that is preferentially pervaporated.

According to solution diffusion model [55], the overall selectivity of pervaporation process α_{WH}^{P} is the product of sorption α_{WH}^{S} and diffusion α_{WH}^{D} selectivity's.

$$\alpha_{WH}^{P} = \alpha_{WH}^{S} \text{ x } \alpha_{WH}^{D} \tag{5.6}$$

Use of Eq. (5.6) is highly restricted as the calculation of sorption selectivity is based on pure component swelling data. Table 5.2 shows the values of selectivity's for different membranes. Further, the selectivity's were plotted against percent ABS in the blended membranes in Fig. 5.4. Fig. 5.4 also includes the selectivity's of all the membranes and shown in inset.

It is clear from Fig. 5.4 that increase of selectivity with increase in ABS percentage in the blended membrane is in the form of sigmoidal growth (essentially there is little variation of selectivity up to 40 % ABS (and perhaps up to a percent of 55) over which there is significant rise in the values of selectivity (70 & 80 % ABS)). However, the inset of Fig. 5.4 which includes polymer EC & ABS shows much lower values of selectivity with its nearest blended membrane. Thus, blended membrane does provide a trend of selectivity with percent composition of ABS.

As mentioned earlier total selectivity is the product of sorption selectivity and diffusion selectivity. Further, sorption and desorption are fast processes whereas diffusion process is slow [7].Accordingly, the diffusion of permeating components through the membrane is the rate determining process. Further, water moves through the membrane faster because of its small size. The speed however increases if the membrane has more hydrophobic character as the binding of water molecules with the membrane will then

significantly decrease. Thus, selectivity should increase with increase in hydrophobic character which was actually noticed in the present case.

However, the membrane BABS2 has lowest selectivity (1.45) among all the membrane. This is because of the smallest thickness (40 μm) of the membrane. Permeability decreased with decreasing membrane thickness as reported by Bode and his associates [56]. The reason for this anomalous behavior was explained on the basis of theory of "membrane resistance at permeate side" as postulated by Cote and Lipski [57].

A more useful term, namely PSI index, was used to analyze membrane performance. PSI index was defined as a product of normalization flux and selectivity. In this study, as there are two different ways to normalize flux there are two PSI indexes which are denoted as $(PSI)_I$ index and $(PSI)_{II}$ index. Eqn. 5.7 & 5.8 define PSI indexes:

$$(PSI)_I \text{ index} = (J)_I \times \alpha_{WH}^P \tag{5.7}$$

$$(PSI)_{II} \text{ index} = (J)_{II} \times \alpha_{WH}^P \tag{5.8}$$

Membranes	*Selectivity*	*(PSI index)$_I$ (kg /m^2.h)x10*	*(PSI index)$_{II}$ (kg^2/m^4.h)x10^3*
EC	1.710	1.650	0.829
BABS1	2.449	3.751	1.766
BABS2	1.450	1.964	0.999
BABS3	1.968	2.743	1.067
BABS4	5.207	2.253	1.260
BABS5	13.237	3.611	2.144
ABS	4.587	3.965	1.884

Table 5.2 – Selectivity and PSI indexes for membranes

In the above Table 5.2, values of PSI indexes are given. PSI indexes were plotted against various membranes and are shown in Fig. 5.5 to 5.6. From Fig. 5.5, it is clear that $(PSI)_I$ index of BABS1 & BABS5 have the highest value. Further, we can say that for dehydration of hydrazine hydrate BASB1 and BABS5 give the higher values of PSI

indexes. However, we are not able to get any definite variation in $(PSI)_I$ index for different membranes. Further, from the plot of $(PSI)_{II}$ indexes with different blended membranes, we get a variation having a minima at around 48 wt % ABS. Thus, we can say that for hydrazine hydrate separation either lower dosage (around 20 %) or higher dosages (around 80 %) of ABS in blended membranes show higher values of PSI indexes. In other words, for hydrazine hydrate separation through PV, a blended membrane of a combination of hydrophilic and hydrophobic characteristics (presently with EC and ABS polymers, respectively) may be suitable but with an imbalanced quantities. Further, the presence of a definite trend also verifies the robustness of assumption of normalization for flux in terms of $(J)_{II}$.

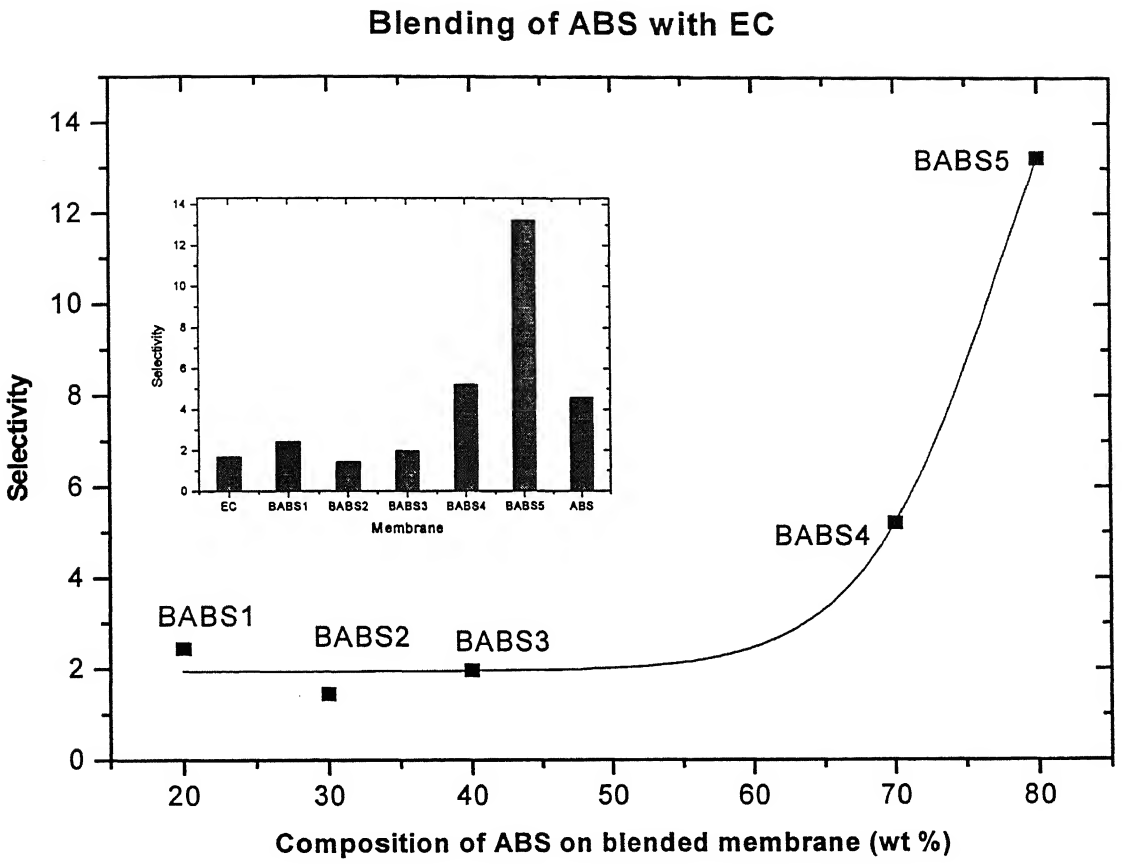

Figure 5.4 - Effect of percentage of ABS in blended membrane on selectivity

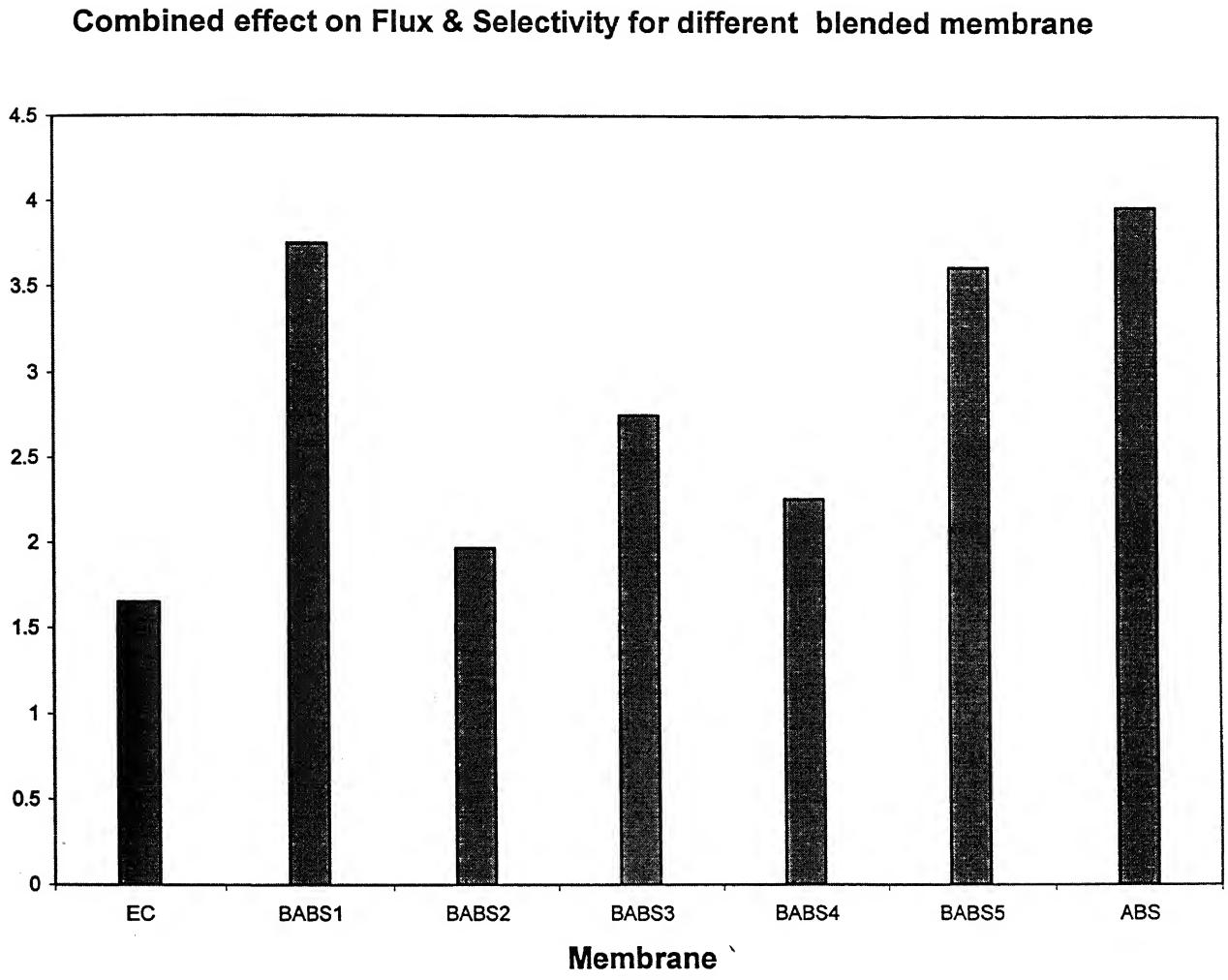

Figure 5.5: $(PSI)_I$ index values obtained for blended membranes

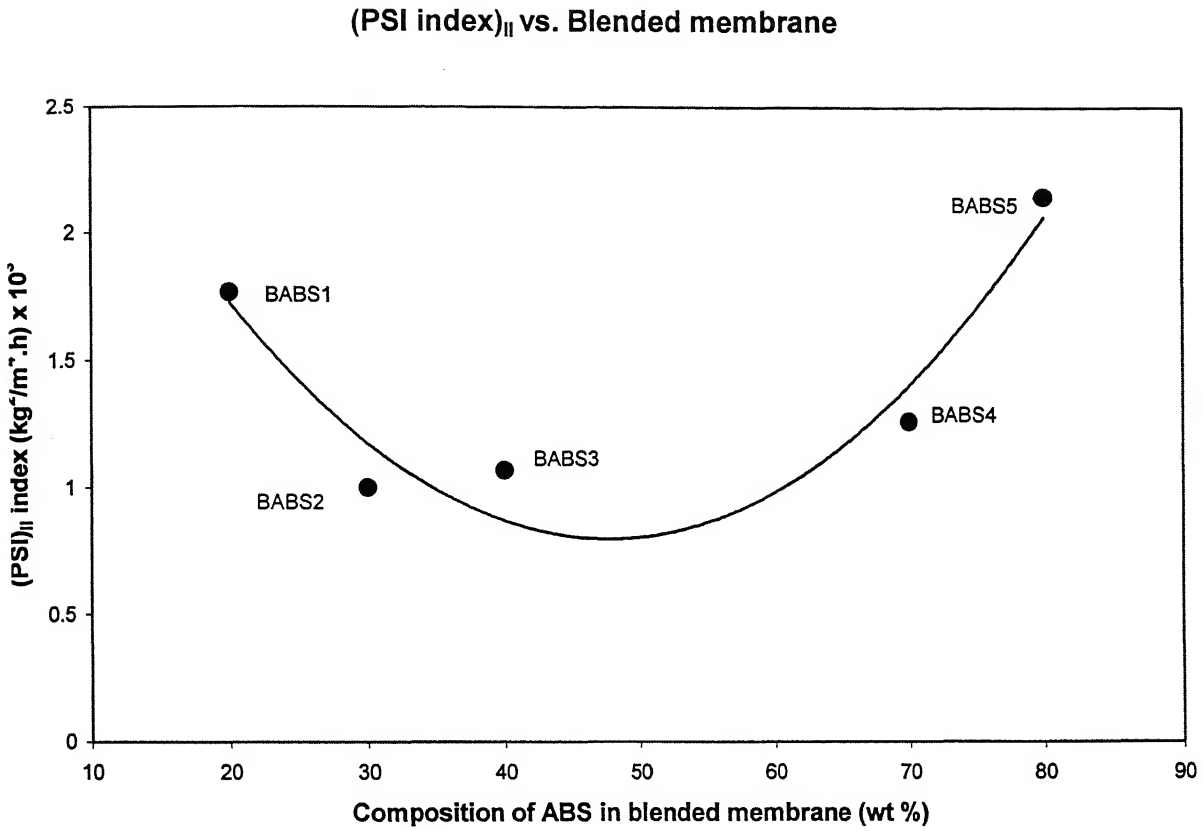

Figure 5.6 - Variation of $(PSI)_{II}$ index with varying composition of ABS in blended membranes

5.2 Characterization of blended membranes

Ethyl cellulose and ABS were blended with different proportions to form blended ABS membrane (BABS). The procedure has been described in the earlier chapter. In the following section, such membranes, however, were characterized in order to observe the modifications in comparison to unmodified form. XRD and positron annihilations techniques were employed for the purpose and results are discussed. Further, contact angles were also measured for the membranes used for the work. Such a restrictive use of characterization techniques (XRD, PAL, Contact angle) were carried out simply to observe the modifications due to blending of ethyl cellulose polymer and ABS polymer.

5.2.1 XRD

The packing of the original and blended ABS membranes were investigated with wide angle X-ray diffraction (WAXRD). WAXRD curves of the membranes were obtained using an Iso-Debyeflex X-ray powder diffractometer having monochromatic radiation of α-rays emitted by Cu at a wave length of 1.54 Å. Scanning was performed with an angle ranging from 6 to 50 at a rate of 3 degree/min with the accelerating voltage of 30 kV and tube current of 20 mA.

WAXRD spectra of ABS and BABS membranes are shown in Fig. 5.7 to 5.11. Both ABS & BABS spectrum's display two sharp peaks at 26° and 32°. The sharp peaks suggest the semi crystalline nature of polymers. However, as EC content increases in the polymer the spectrum's shows variation in intensity at low angle range (between 6 -20). Qualitatively, this change suggests that the blended ABS membranes are slightly more amorphous compared to ABS membrane. Further, this amorphous character increases when EC content increases in the blended membrane. This may, in a sense increase the flux. Further, studies on XRD spectra, particularly of detailed structures of the polymers, are insignificant for the present work.

Figure 5.7 - XRD spectrum of ABS membrane

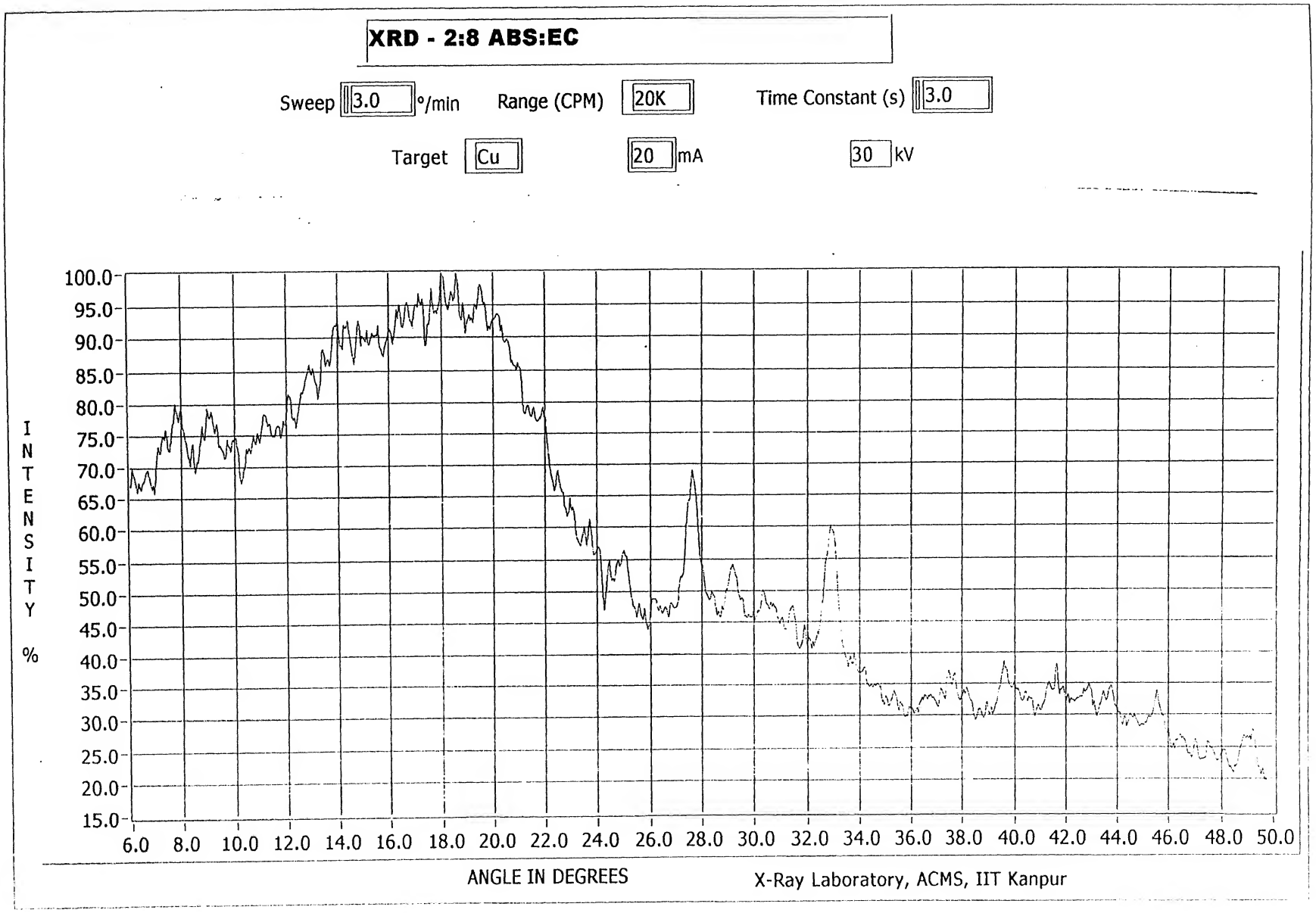

Figure 5.8 - XRD spectrum of BABS1 membrane

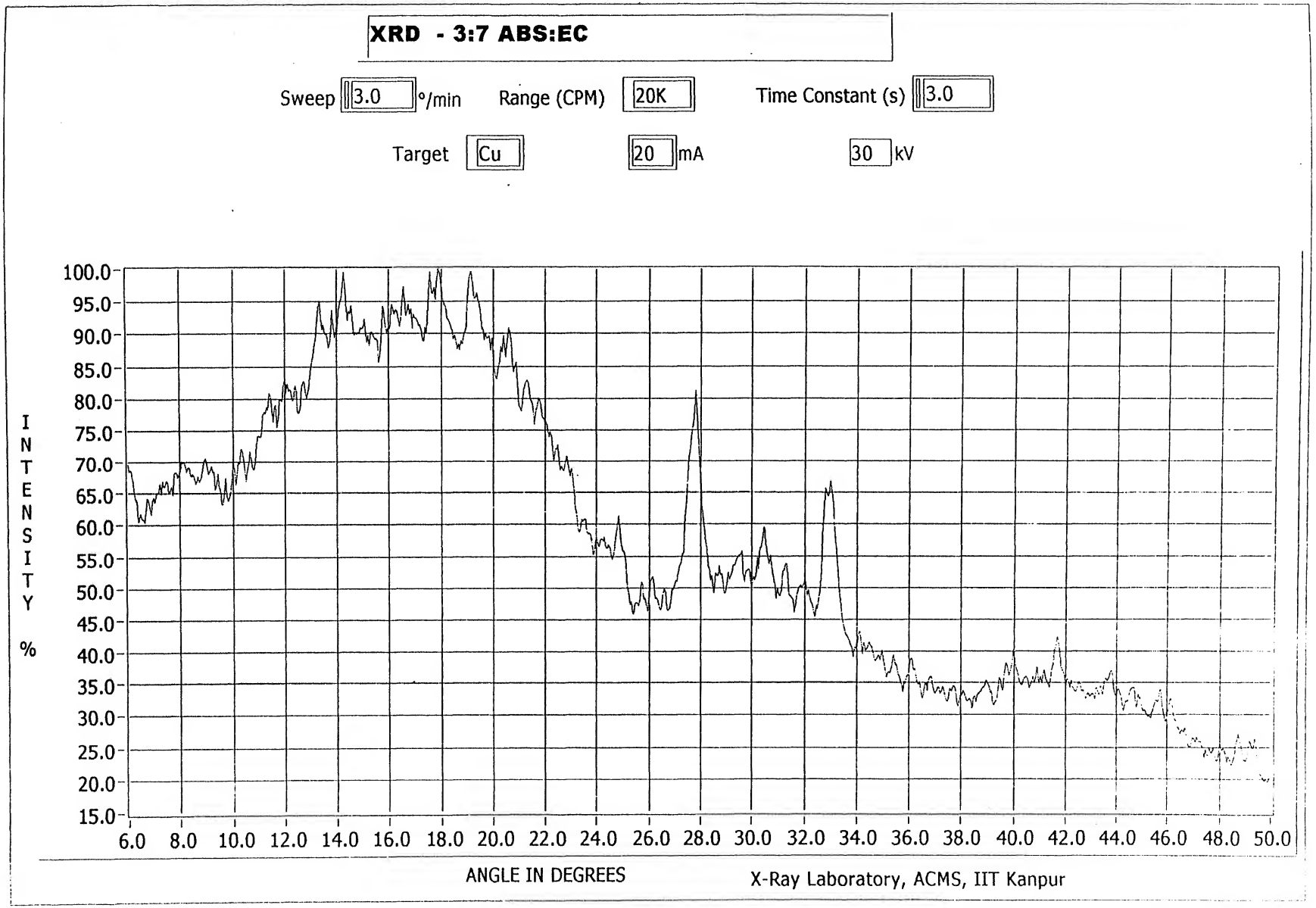

Figure 5.9 - XRD spectrum of BABS2 membrane

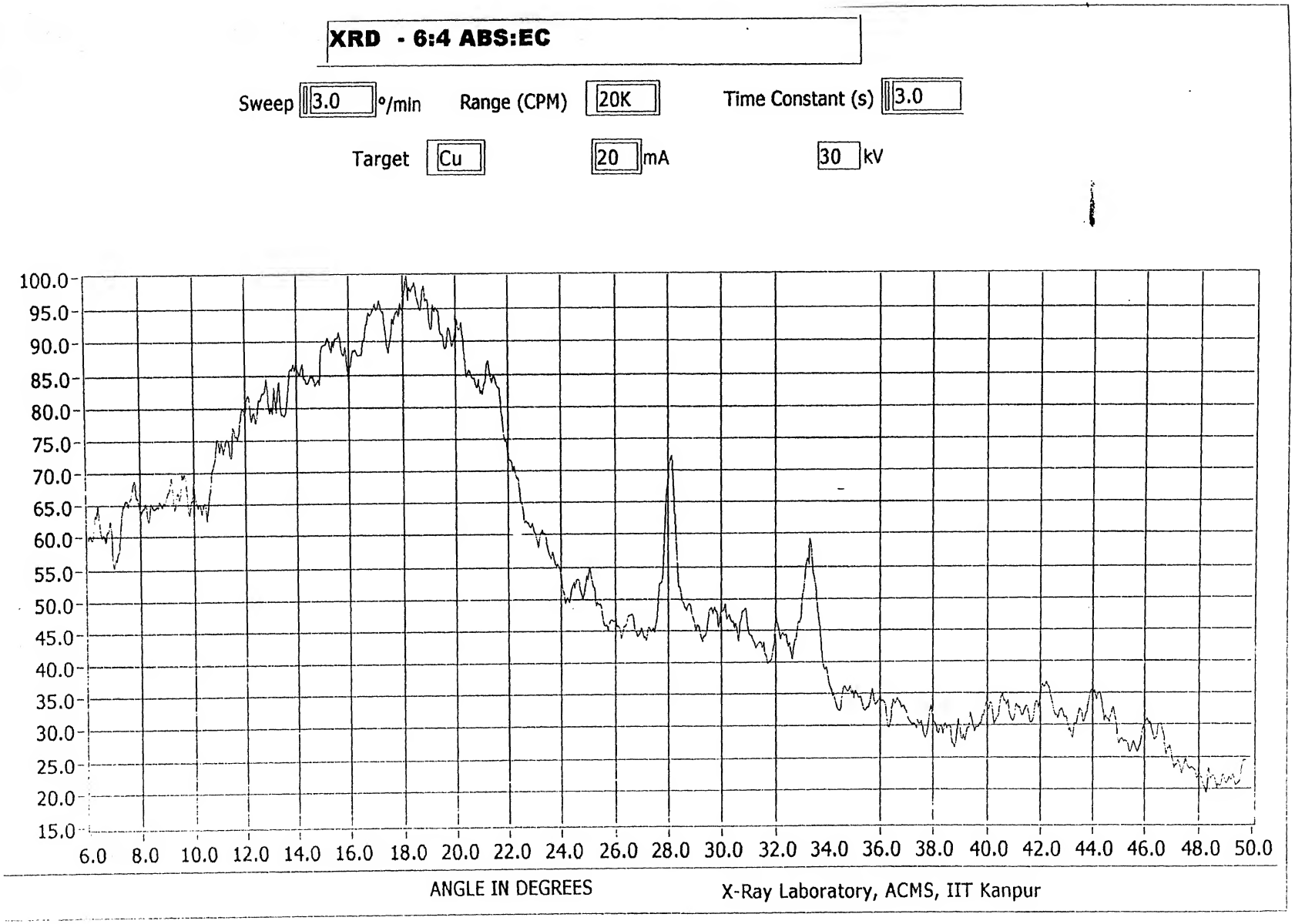

Figure 5.10 - XRD spectrum of BABS3 membrane

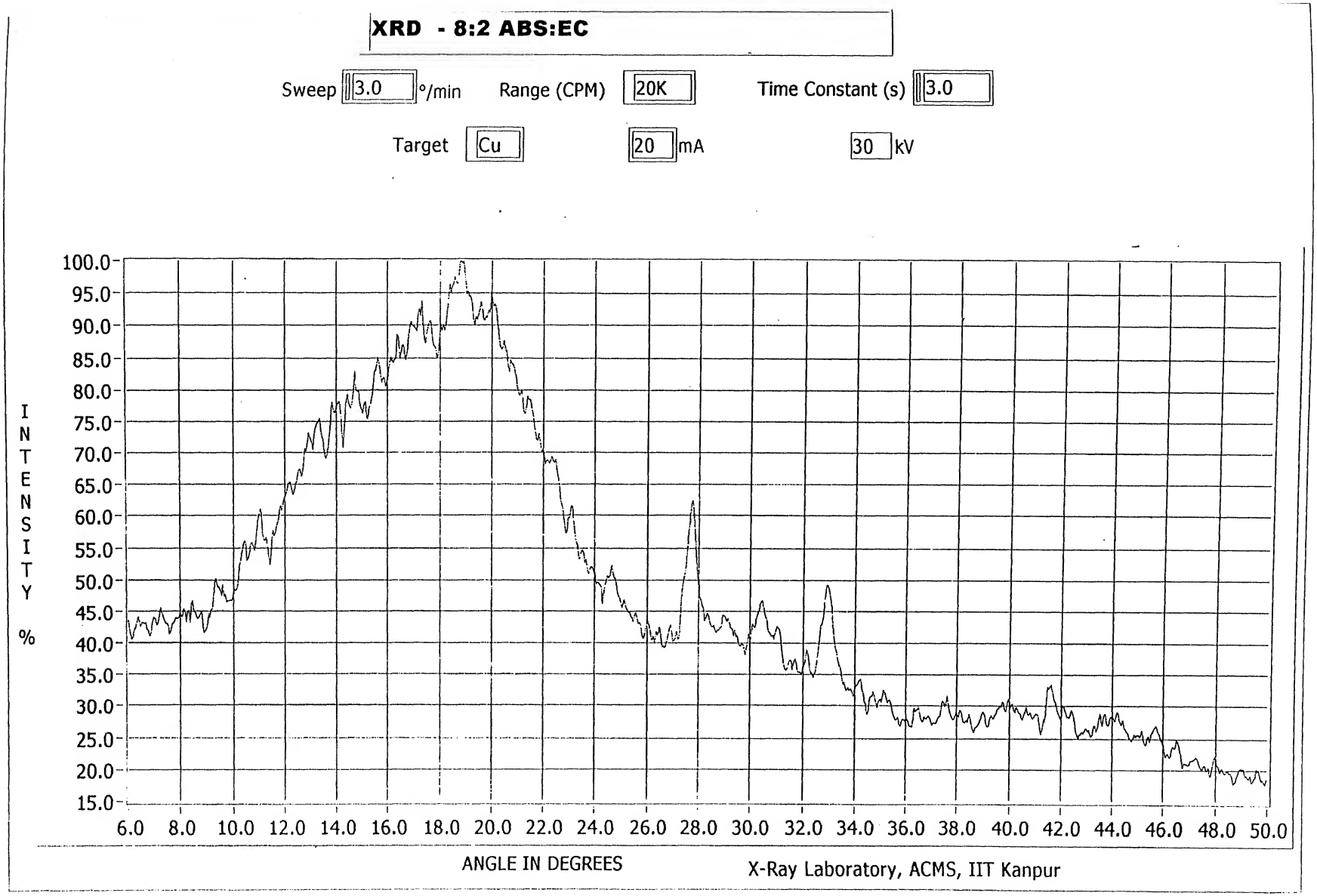

Figure 5.11 - XRD spectrum of BABS5 membrane

5.2.2 Positron Annihilation Lifetime (PAL) Spectroscopy

The PAL measurements were carried out using a fast-fast system having a resolution of 300 pico-seconds (FWHM for the ^{60}Co prompt γ-rays, under ^{22}Na window settings). The positron source was prepared by depositing around aqueous 2 micro-Curie solution of $^{22}NaCl$ on a thin aluminium foil (thickness ~ 12μm) which was covered with an identical foil. Approximately, one million counts were collected in each spectrum and four spectra were measured for each sample. The lifetime data were analyzed using PATFIT-88 programs [58]. Source correction was done for all the spectra. The following expression was used to relate o-Ps pick-off lifetime (τ_3) and special free volume radius (r) [45].

$$\tau_3 = \frac{1}{2}\left[1 - r/(r+\Delta r) + \left(\frac{1}{2\pi}\right)\sin\left(\frac{2r\pi}{r+\Delta r}\right)\right]^{-1} \tag{5.9}$$

Where, Δr is the electron layer thickness. Further, the fractional free volume f, may be estimated from the following empirical relation.

$$f = bV_F I_3 \tag{5.10}$$

Where, V_F is the free volume of the membrane and I_3 is the intensity corresponding to τ_3. The scaling factor b, is obtained from variation of free volume with temperature. However, in the absence such data, it may be typically assigned a value of $1.0/nm^3$ [48].

Section 3.4.4 describes the detailed work on positron lifetime spectroscopic analysis made for varieties of dense membranes in order to obtain primarily free volume parameters. In this section, results pertaining to ABS and modified ABS membranes are presented in Table 5.3 to observe the modification of the same. Ortho positron lifetime (τ_3) values were observed to be smaller for blended membranes compared to pure EC & ABS membrane. Further, the intensity values steadily decreases from BABS1 to BABS5. Further, it also shows the calculated values of free volume fraction which was also found to be slightly smaller for blended membranes as compared to EC and ABS. These obtained free volume parameters are in general in the same range as given for semi crystalline polymers [59]. Therefore, during blending of ethyl cellulose with ABS, free volume becomes smaller and this may lead to decrease of species diffusivities within membranes which eventually reduce flux for BABS-4 & 5 membranes than that of ABS membrane.

Membrane	*State*	τ_3 *(ns)*	I_3 *(%)*	*r (nm) (sphere)*	V_f (nm^3)	*f*
EC	Dry	2.63	22.5	0.33	0.150593	0.034
BABS1	Dry	2.26	23.9	0.30	0.113143	0.027
BABS2	Dry	2.26	23.1	0.30	0.113143	0.026
BABS3	Dry	2.26	-	0.30	0.113143	-
BABS4	Dry	2.28	20.2	0.294	0.106489	0.022
BABS5	Dry	2.23	21.2	0.29	0.102202	0.022
ABS	Dry	2.54	21.1	0.32	0.137314	0.029

Table 5.3 - Positron annihilation parameters and respective free volume parameters of blended membranes

5.2.3: Contact angle analysis

Contact angles of water were measured on different blended membranes and the results were tabulated in Table 5.4.

Membrane	*Water contact angle (degree)*
EC	61.600
BABS1	65.157
BABS2	66.340
BABS3	68.560
BABS4	72.430
BABS5	77.040
ABS	88.988

Table 5.4 - Values of Contact angles of water on different membranes

The contact angles of water on blended membranes as well pure polymeric EC & ABS membranes were studied in Fig. 5.12. It may be observed from Fig. 5.12 that with increase in ABS composition (from left to right) the contact angle is increasing exponentially. This suggests that when ABS content in a polymer increases the hydrophobicity of the polymer also increases. Thus, expectedly, EC membrane on blending with ABS (MEC4 membrane) changes its characteristics from hydrophilic to hydrophobic, as evidenced from increase of contact angle.

Further, Fig. 5.13 depicts relationship between process selectivity (for blended membranes) and contact angles of water in membranes. It is clear from Fig. 5.13 that increase in ABS percentage in the blended membrane exponentially increases the selectivity value of dehydration of hydrazine hydrate. Further, following exponential relationship was developed with correlation coefficient of 0.9824.

$$\text{Selectivity} = [3.73\text{x}10^{-6}].\exp(\theta/5.11) \qquad (5.11)$$

where, θ is the contact angle of water in blended membrane. This may prove useful to estimate selectivity for blended polymers of unknown pervaporation performance but known contact angles.

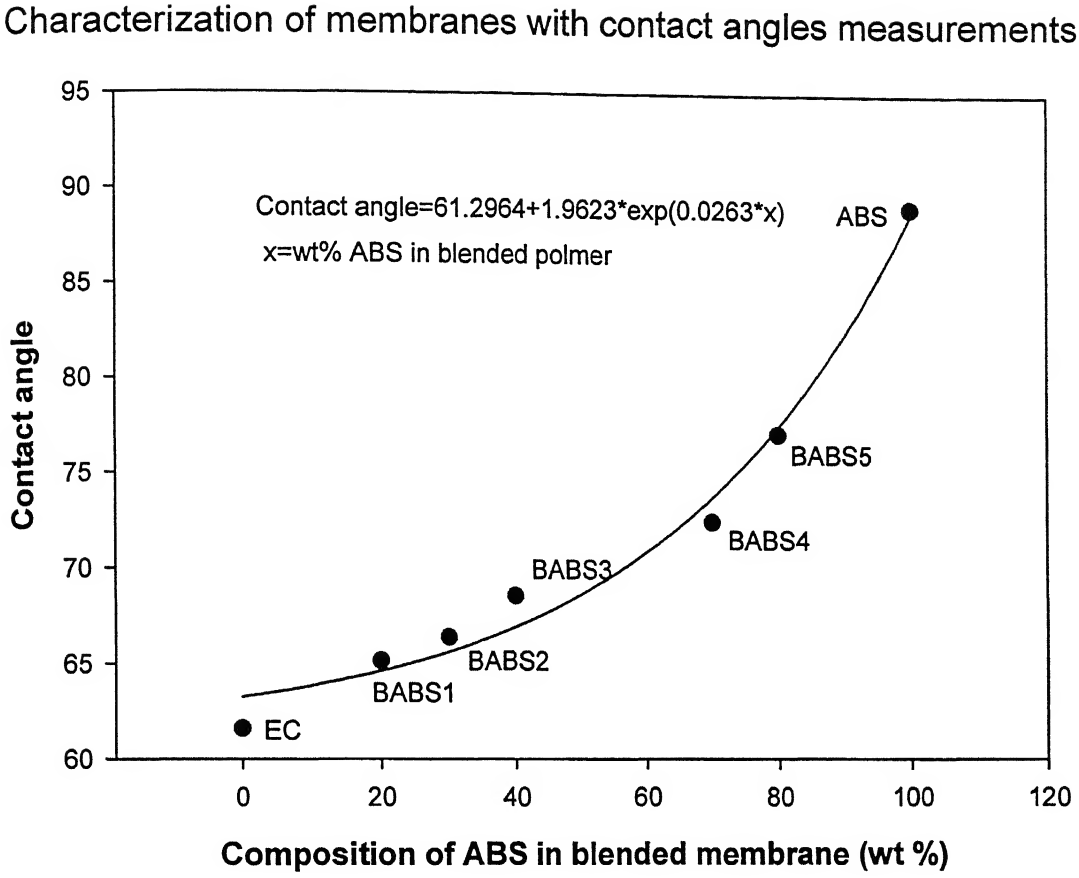

Figure 5.12 - Variation of contact angle for varying composition of ABS in blended membranes

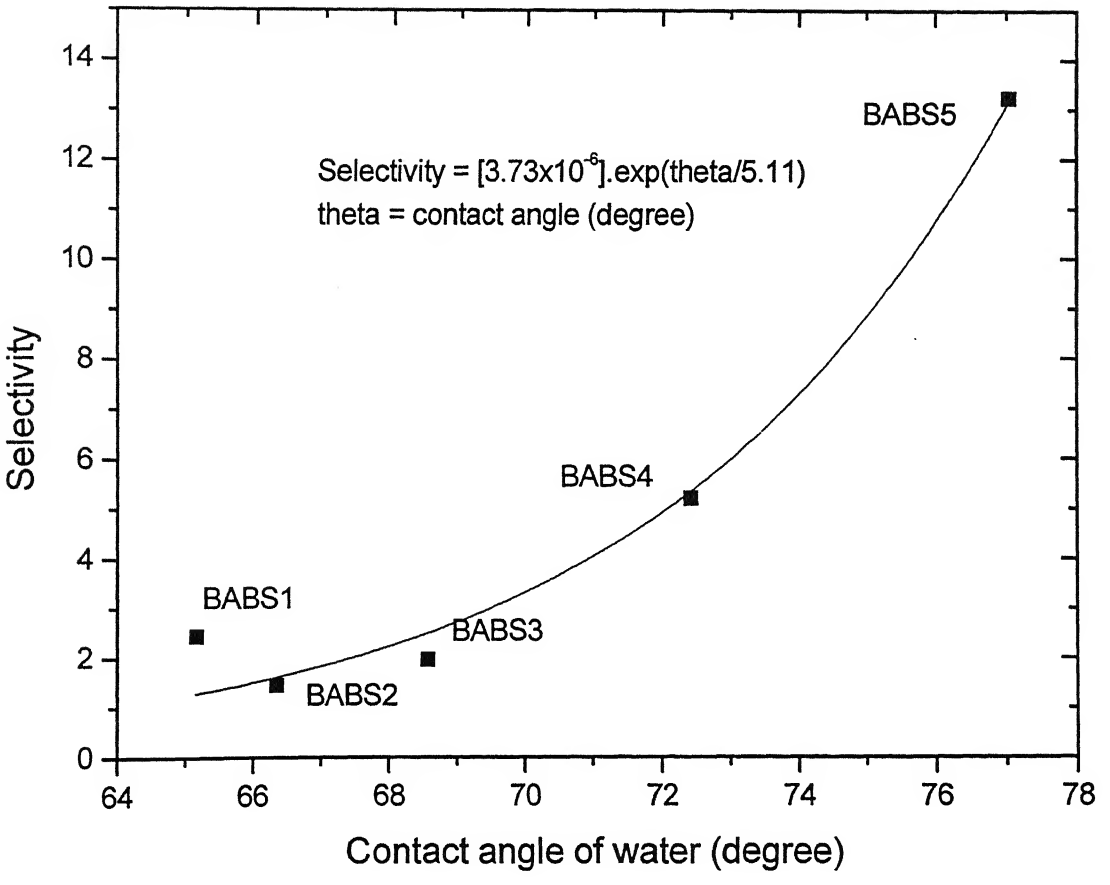

Figure 5.13 – Variation of Selectivity for varying contact angles (water)

5.3 Sorption study of blended ABS & EC membranes

5.3.1 Pure component sorption

Pure component sorption studies were carried out at 50^0C (for water) for different blended as well as pure polymeric membranes to get the equilibrium weight fraction of permeant. Fig 5.14 shows the change of sorbent weight fraction within membrane phase with time. This figure depicts that sorbent concentration within the phase is coming to a constant value after around 24 hours. Therefore, this sorption concentration was taken as equilibrium concentration of sorbent. Further, the sorption experiment was carried out upto 72 hours and the trends are found to be linear. The values cof this sorption experiment are given in Appendix D.1.

5.3.2 Binary component sorption

Sorption experiments were conducted on different blended membranes using hydrazine hydrate solution at 50 °C. Fig. 5.15 depicts the variation of sorbent concentration against time for various membranes. Interestingly, for all the membranes equilibrium concentration was coming also around 24 hours (values are given in appendix D.2).

Further, the equilibrium sorption values for both water and hydrazine hydrate system are reported in Table 5.5. Interestingly, equllibrium sorption values for hydrazine hydrate is higher than water for every mambranes. Similar attribution was made for EC membarne by Ravindra et al. [7].

Membrane	*% Sorption of water (g/g of dry polymer)*	*% Sorption of hydrazine hydrate (g/g of dry polymer)*
EC	4.12	5.23
BABS1	2.20	4.56
BABS2	1.12	8.21
BABS3	0.59	4.81
BABS4	1.31	4.53
BABS5	2.67	5.97
ABS	0.31	0.50

Table 5.5 – Experimental results for sorption of water and hydrazine hydrate

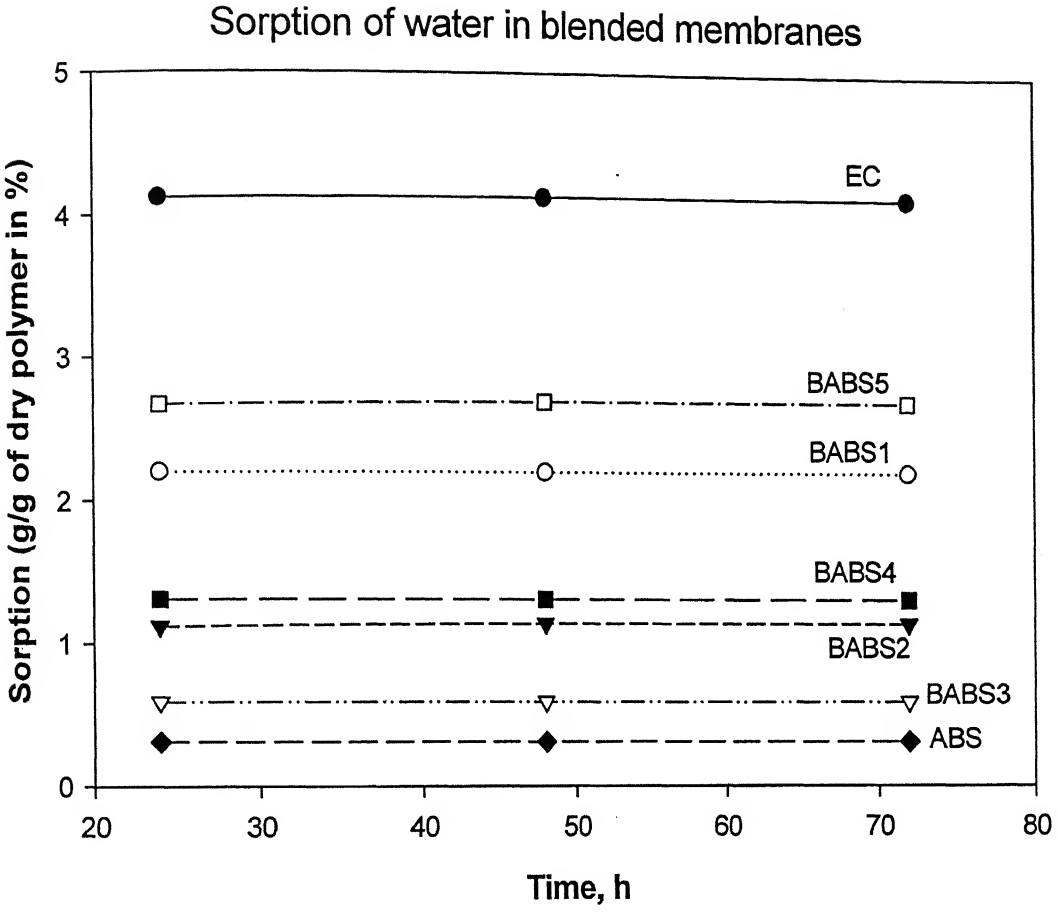

Figure 5.14 - Sorption of water as a function of time for blended membranes

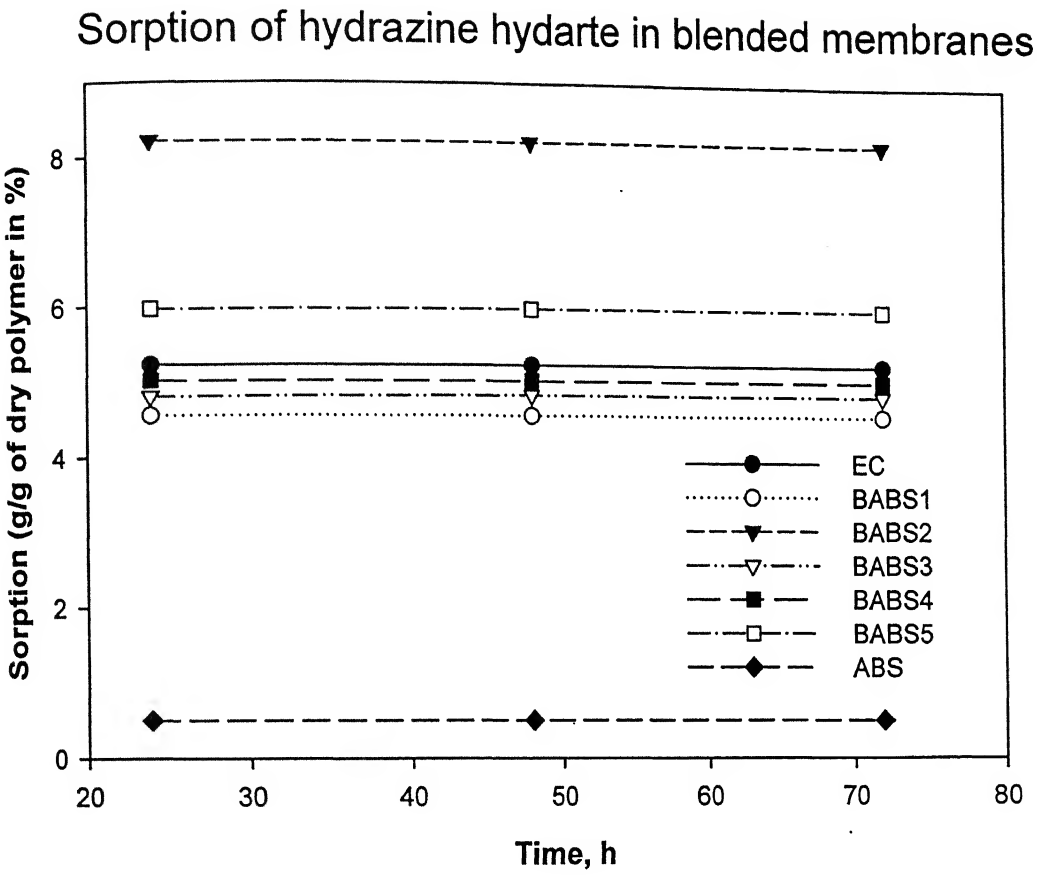

Figure 5.15 - Sorption of hydrazine hydrate as a function of time for blended membranes

5.4 Separation study of Modified PS membranes

In the present work, modification of hydrophobic polystyrene (PS) polymer was also contemplated by introducing sulphonic acid groups (through sulphuric acid reaction) to increase hydrophilicity of the polymer. This approach was earlier utilized in a recent work [10] where ethyl cellulose polymer was modified by introducing carbamate groups (reacting ethyl cellulose with phenyl iso-cyanate) to increase hydrophobicity of the polymer. The modification process was earlier discussed in section 4.3.3. In all cases, 1 hour of sulphonation time was used. The salient results of pervaporation process of hydrazine hydrate system using different sulphonated membranes will be discussed in this section.

5.4.1 Influence sulphonation in modified membrane on Flux

The effects of sulphonation on permeation rate and product concentration were studied by keeping other parameters constant (temperature: 50°C, downstream pressure: 0.1mmHg, static feed condition). The permeate flux ($kg/m^2.h$) was calculated using equation 5.1, as discussed in earlier section. As the membranes are of varying thicknesses, the values of flux are normalized for affixed thickness (5μm) using equation 5.2 and denoted as $(J)_l$. The values of flux, normalized flux & thickness are tabulated in Table 5.6.

Membrane	*Thickness* $(m)x10^6$	*Flux* $(kg/m^2.h)x10^3$	*Normalized Flux,* $(J)_l$ $(kg/m^2.h)x10$
MPS0	90	7.282	1.311
MPS1	85	9.425	1.602
MPS2	90	10.402	1.872
MPS3	85	11.591	1.971
MPS4	90	18.328	3.299

Table 5.6 – Experimental and normalized values of flux obtained for sulphonated PS membranes along with thickness

The experimental flux and normalized flux [$(J)_I$] are plotted against concentration of sulphuric acid (used for sulphonation) in Fig. 5.16 & 5.17. From Fig. 5.16, one may observe that with increase in sulphuric acid concentration the flux increases exponentially. However, when one plots normalization flux, $(J)_I$ against sulphuric acid concentration, an exponential increase of $(J)_I$ with increase in sulphuric acid concentration is observed.

The polymer PS is a strong hydrophobic polymer (contact angle value in water reported [10] to be 79). Further, SO_3H^- group is a strong hydrophilic group. Thus, with the increase in quantity of SO_3H^- group in the polymer chain the hydrophilicity of the polymer may also increase. The percentage of sulphonation of the polymer increases if one uses higher concentration of sulphuric acid, keeping other variables (temperature: 35° C, sulphonation time: 1hour) constant. Similar attributions were also made by Akovali and Ozkan [50]. Thus, it may be concluded that the flux increases as hydrophilic property of the membrane increases.

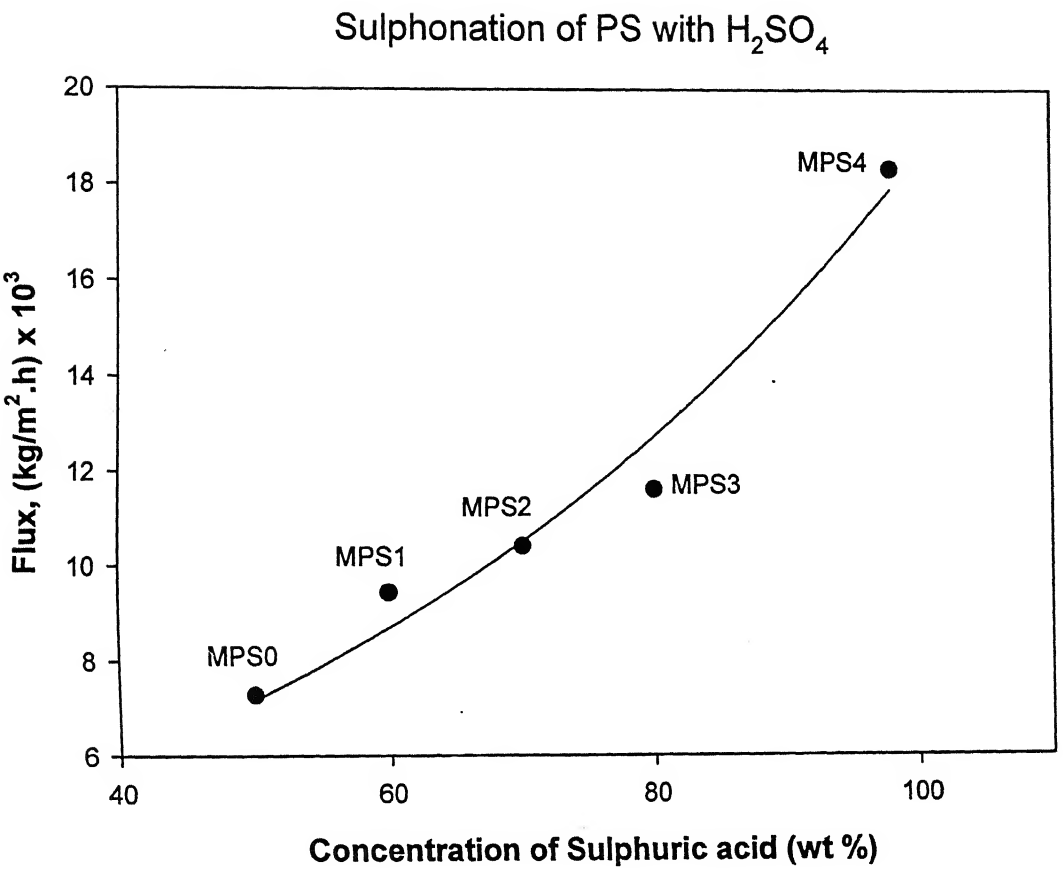

Figure 5.16 - Flux for different sets of modified membranes obtained with varying concentration of H_2SO_4

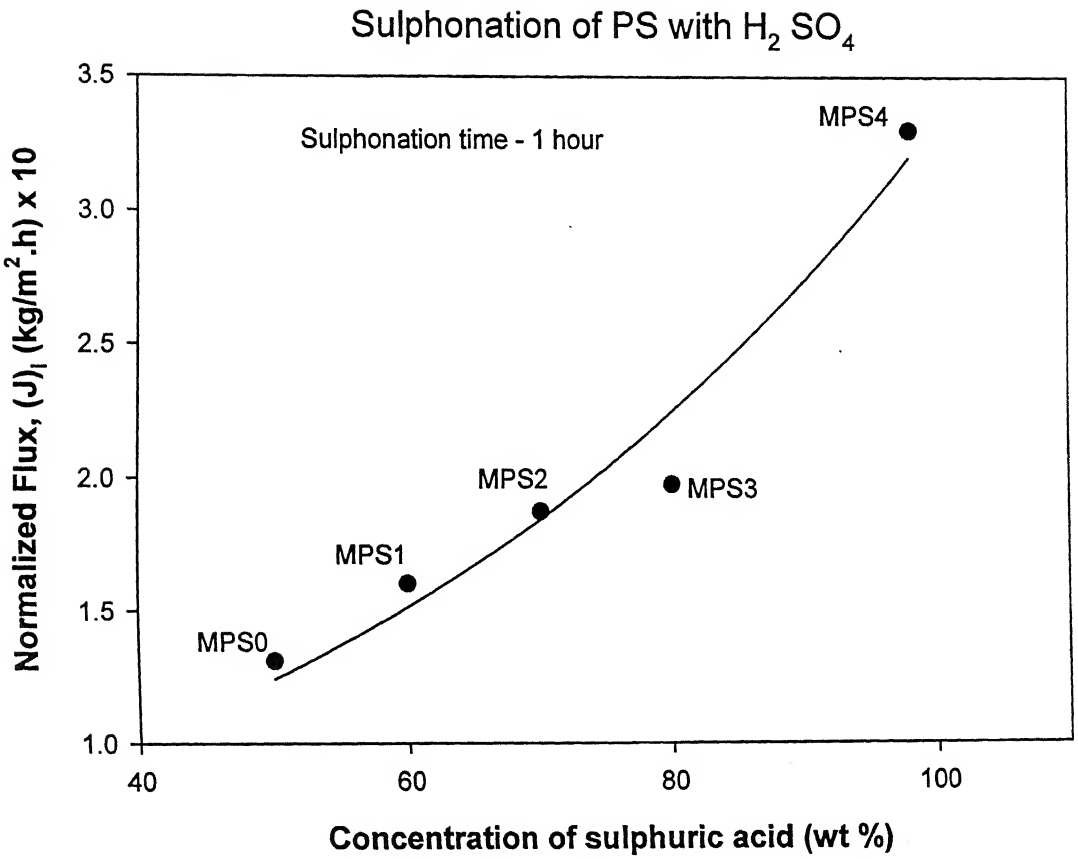

Figure 5.17 – Normalized Flux for different sets of modified membranes obtained with varying concentration of H_2SO_4

5.4.2 Influence of sulphonation in modified membrane on selectivity & PSI index

To observe effect of sulphonation on dehydration of hydrazine hydrate, pervaporation selectivity's have been measured using equation 5.5. Further, PSI index were also measured using equation 5.8. The theories behind these equations have already been discussed in the previous sections. The values of selectivity and PSI index are tabulated in table 5.7. Further, the selectivity's for different membranes (denoted in the graph) are plotted against concentration of sulphuric acid and shown in Fig. 5.17. It may be observed from figure 5.18 that selectivity's decreases exponentially with increase in weight percent sulphuric acid, used for sulphonation. As discussed earlier, diffusion selectivity decreases with increasing hydrophilicity. Further, with increase in sulphuric acid concentration (for sulphonation) the hydrophilicity of the membrane increases. Thus membranes MPS1, MPS2, MPS3 and MPS4 are more hydrophilic from 1 to 4. Thus selectivity should decrease from MPS-0 to 4 and indeed such observation is noticed in the present case.

Membrane	*Selectivity*	*PSI index* $(kg/m^2.h)x10$
MPS0	3.162	4.145
MPS1	2.870	4.599
MPS2	2.523	4.724
MPS3	2.295	4.522
MPS4	1.298	4.284

Table 5.7 – Selectivity and PSI indexes for membranes

Fig. 5.19 describes the PSI index values with different sulphonated membranes. Further, from the plot one can visualize that the PSI index values of MPS1, MPS2, and MPS3 are higher compared with other membranes. Again MPS2 has highest PSI value and it corresponds to 70% sulphuric acid. Further, the plot also passes through maxima around 68%. Thus, one may conclude that for dehydration of hydrazine hydrate a

balanced dosage of suphuric acid may be required to carry out sulphonation which may produce a useful sulphonated - PS membrane, as evident from results.

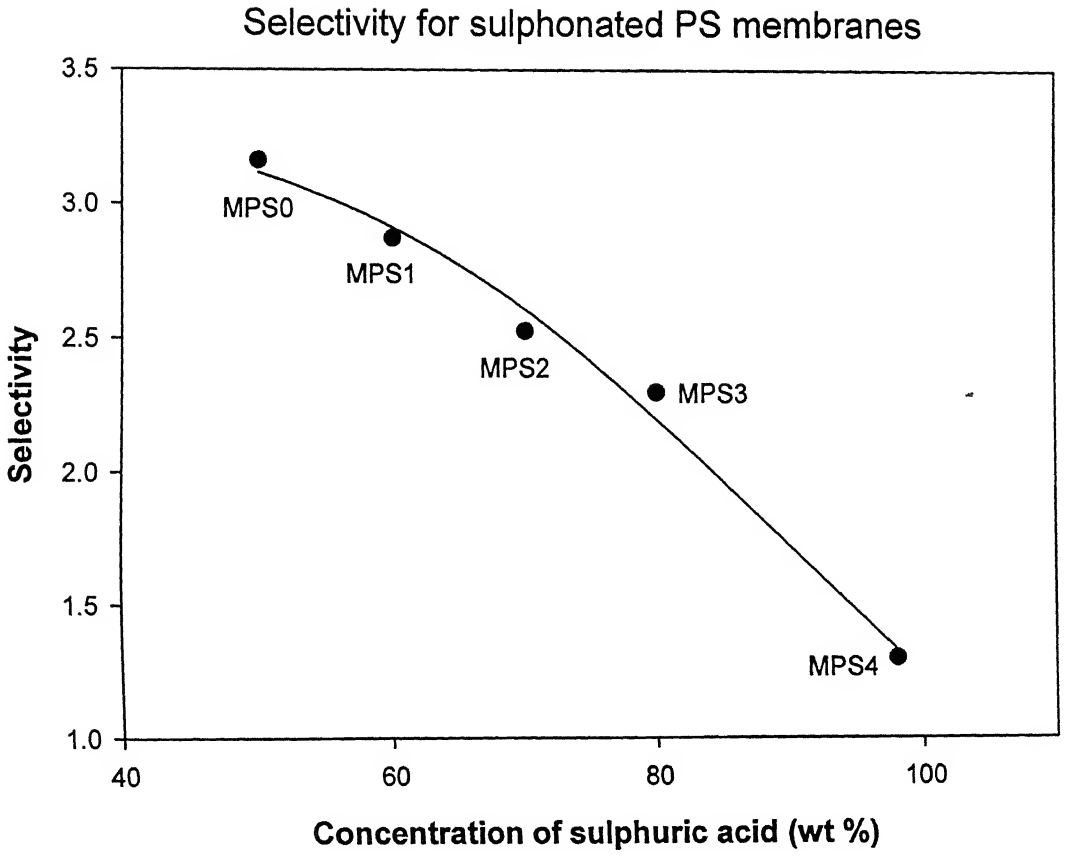

Figure 5.18 - Selectivity for different sets of modified membranes obtained with varying concentration of H_2SO_4

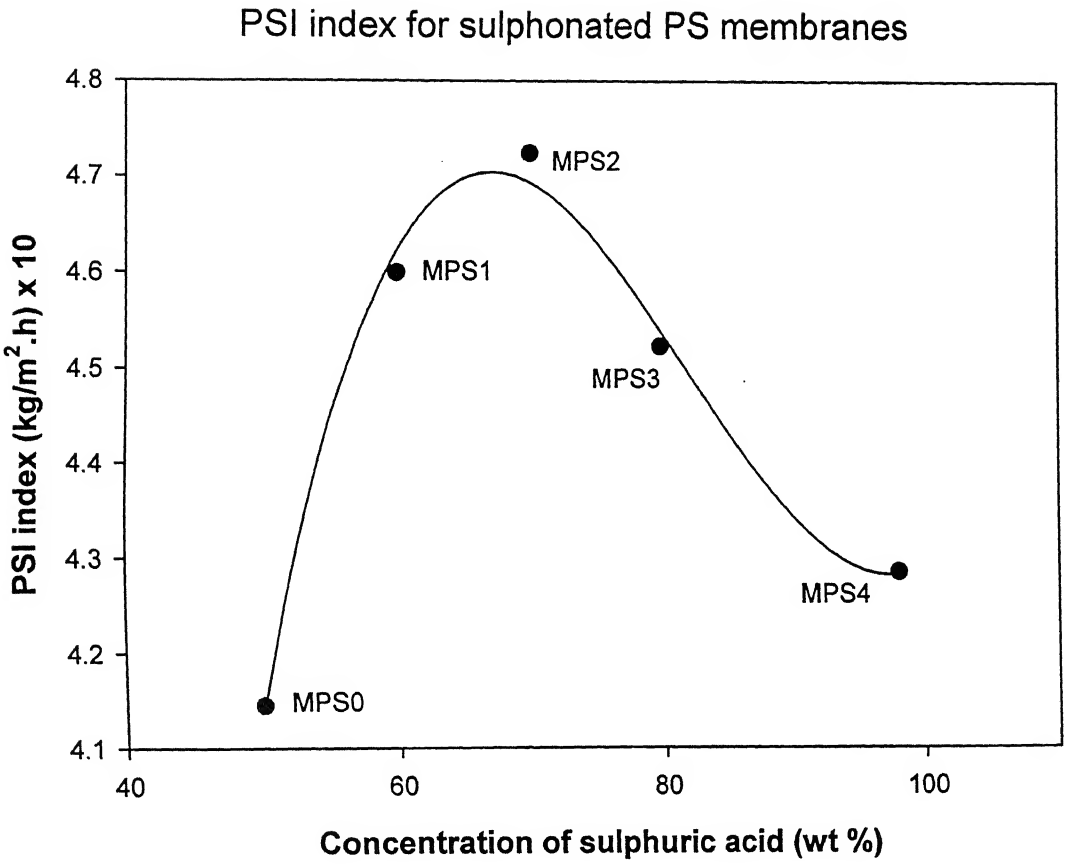

Figure 5.19 – PSI index for different sets of modified membranes obtained with varying concentration of H_2SO_4

5.5 Characterization of modified membranes using FT-IR technique

The FT-IR spectra of the MPS4 membrane was obtained with a Bruker vector 22-spectrometer. The membrane was first diluted in di-chloro methane solvent and was deposited on germanium IR window. The solution forms a thin film upon evaporation of solvent. All FT-IR spectra represent an average of 256 scans with a frequency resolution of 2 cm^{-1} and frequency range of 3000 – 600 cm^{-1}. The obtained spectrum is shown in Fig. 5.20 (1600 - 500 cm^{-1}) and 5.21 (3000- 2000cm^{-1}).

The SO_3^- group anti-symmetric and symmetric vibrational adsorption peaks can be assigned to the peaks 1134.84 and 995.91 cm^{-1}, respectively [60]. Orler et al. [61] have also observed peaks of 1128 and 1097 cm^{-1} for confirmation of sulphonation. Though, we didn't get a peak at 1097 cm^{-1}, a peak was however observed around 1134 cm^{-1} (near 1128 cm^{-1}) which is sufficient enough to confirm sulphonation of PS. Further, at lower wave number range, the peaks of 701.92 & 745.14 cm^{-1} are characteristics bands for PS's (out of skeleton bending vibration of benzene ring [62] and out of plane bending vibration of the five –CH- groups in the benzene ring). Thus, these two bands, especially the band at 701 cm^{-1} correlate sulphonation degree [60]. Further, lower the sulphonation degree; the greater will be the intensities of these bands. Estimation of degree of sulphonation for various sulphonated PS membranes may be a task for future work in this direction along with their relative separation characteristics.

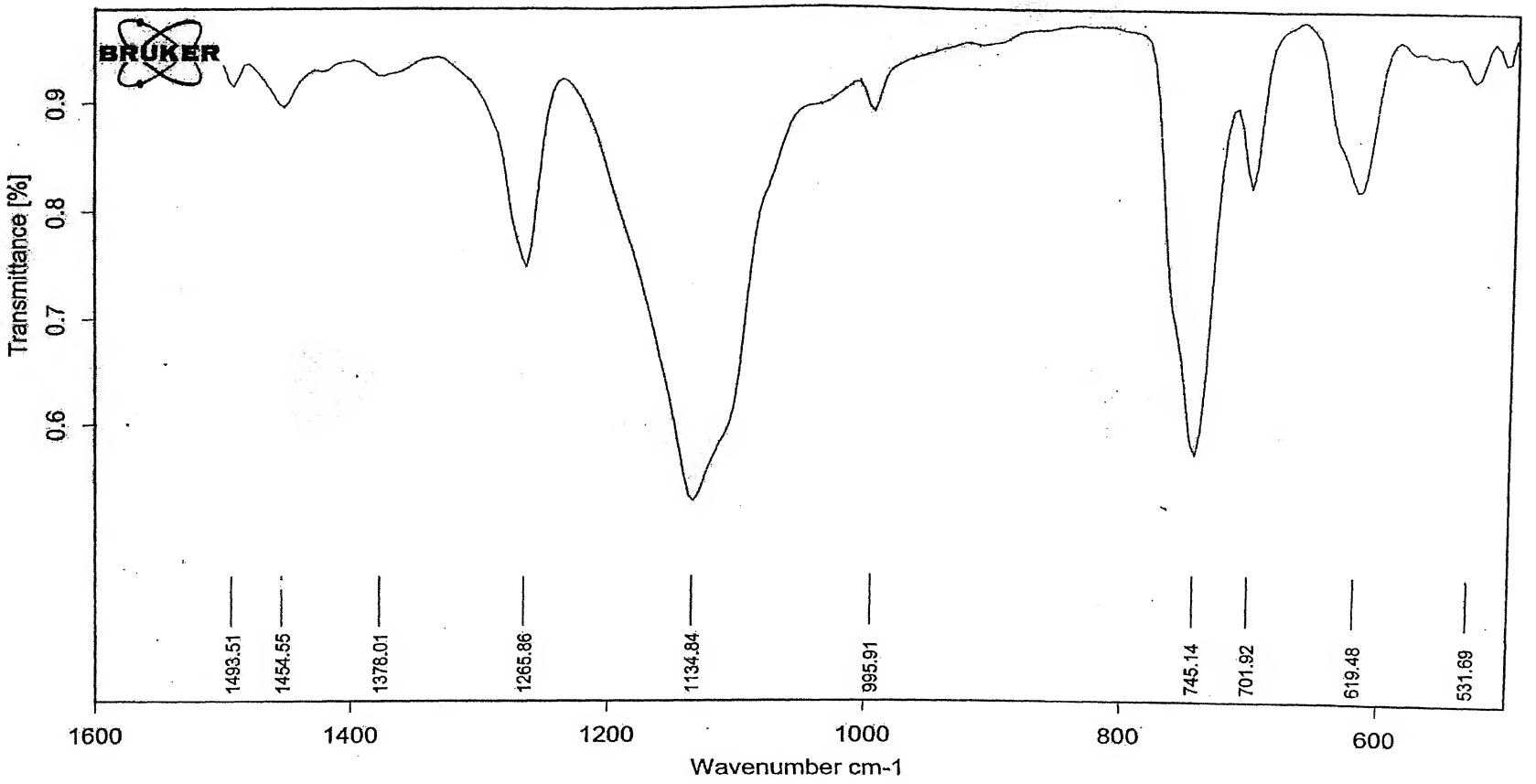

Figure 5.20 – FT-IR spectrum of MPS4 membrane (1600 – 500 cm^{-1})

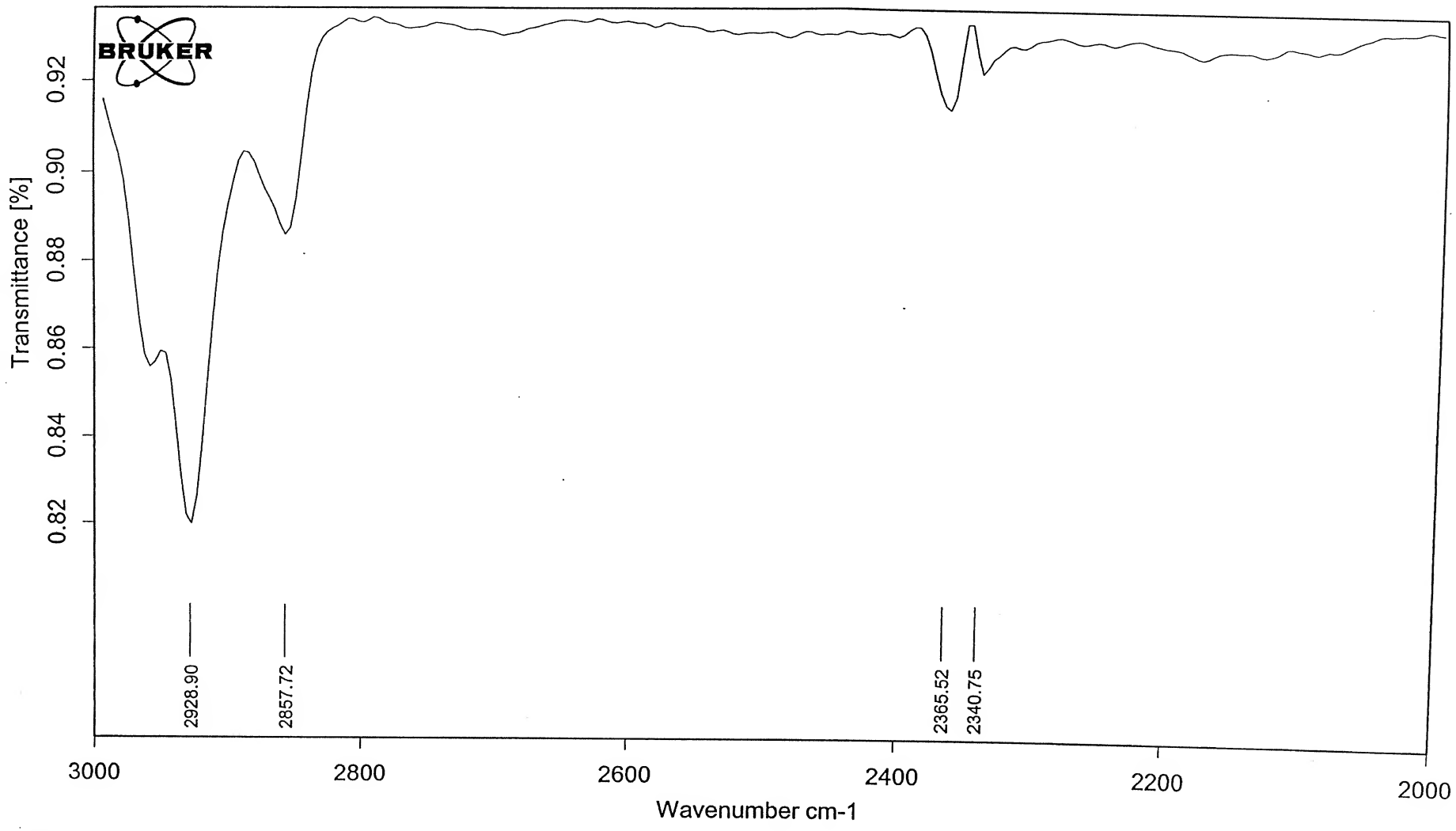

Figure 5.21- FT-IR spectrum of MPS4 membarne (3000 -2000 cm^{-1})

C:\OPUS_NT\MEAS\PSSA.0 sample form 13/04/2004

Chapter 6

Conclusions

Separation of hydrazine-water was carried out using various blended (EC & ABS) as well as pure EC and ABS membrane. Further, PS membrane was modified by reacting with sulphuric acid at varying concentrations. The membranes thus obtained were characterized with the help of FTIR, XRD, PAL and contact angle measurements. Pervaporation experiments were carried out and the results were analyzed with the help of sorption experiments and contact angle measurements. Following conclusion may be drawn based on the results & discussions.

1. XRD analysis suggested blended ABS membranes are slightly more amorphous compared to ABS membrane. This amorphous character increases with increasing EC content in the blended polymer. This may, in a sense increase the flux.
2. Contact angle measurements ascertained that the blending of EC with ABS, increases hydrophobic characteristic with increasing ABS content.
3. Positron annihilation technique successfully estimated free volume fraction, which reduced significantly upon blending. This may lead to decrease in flux in blended membranes which was actually noticed between BABS-4 &5 and ABS membrane.
4. FTIR spectrum analysis confirms the sulphonation of PS for the reaction of Sulphuric acid with Polystyrene.
5. Pervaporation of hydrazine hydrate experiments provided encouraging results in terms of obtaining higher selectivities (as high as 13. 24) than the one that could be achieved through conventional distillation (1.4 at 760 mmHg [2]).
6. PSI index suggested sulphonation of polystyrene produce better membranes for dehydration of hydrazine hydrate than blending of EC with ABS.

7. For hydrazine hydrate separation through PV, a blended membrane of a combination of hydrophilic and hydrophobic characteristics (presently with EC & ABS polymers, respectively) may be suitable but with an imbalanced quantities.
8. Sorption studies suggested that hydrazine has greater affinity towards blended as well as pure EC and ABS membranes. This may actually decreases the permeation of hydrazine through these membranes.

Chapter 7

Recommendations

Based on the work carried out for the pervaporative separation hydrazine hydrate system, several experiences were gained, some of which are listed below as recommendations for future work.

1. Future work should be done to measure degree of sulphonation in the sulphonated membrane. Mass spectra and H NMR spectra may be obtained in this regard.
2. Pure component sorption studies on hydrazine for different blended membranes may be carried out to quantitatively measure sorption selectivity and therefore diffusion selectivity for the above membranes.
3. FT-IR and DSC studies on different blended membranes may be carried out for better understanding of bindings of these molecules (water & hydrazine) with the membrane.
4. Further, a model can be predicted from the different values of flux and selectivity's obtained.
5. Future experiments may be carried on these blended membranes using different temperatures, feed concentration and in continuous mode.
6. Improved method for casting (Automatic Film applicator) may be used to rectify the variation in thickness in evidently obtained in our case.

Appendix

Appendix A

A.1 G.C Calibration of hydrazine hydrate system

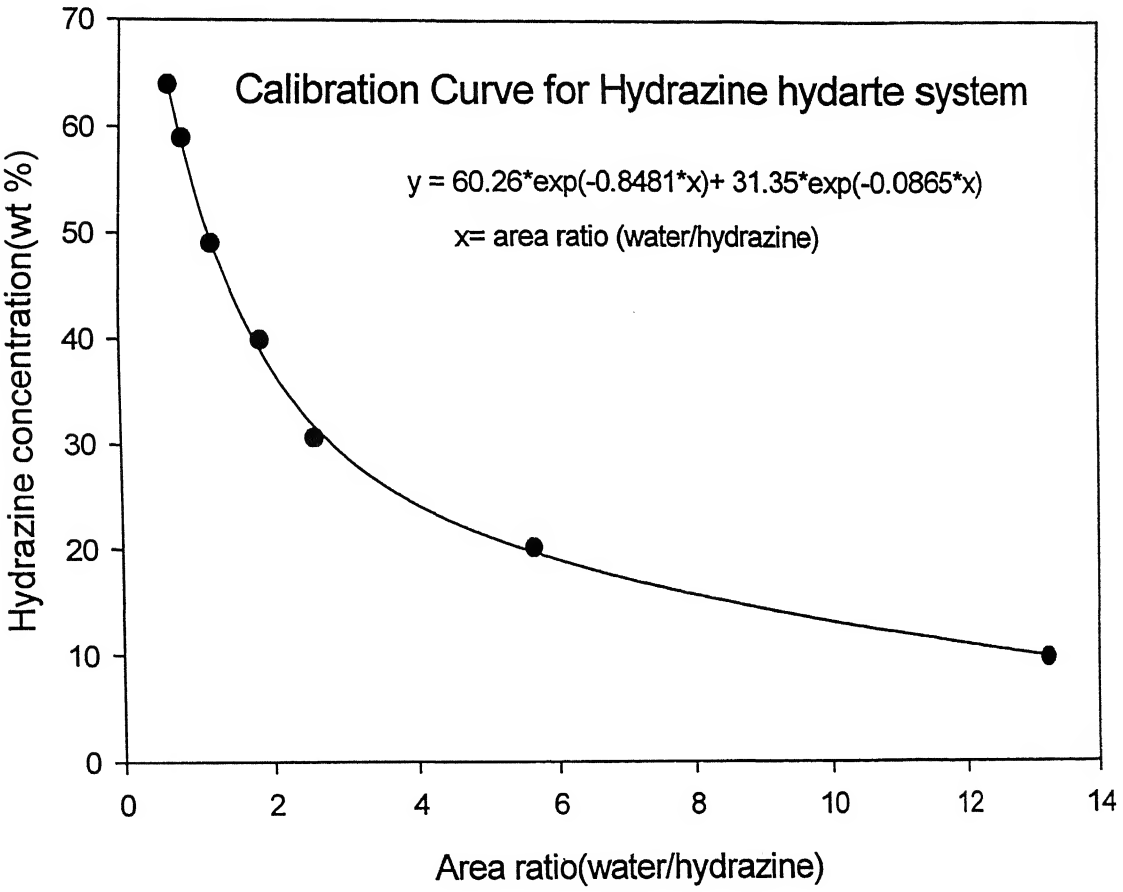

Fig A.1.(a) G.C Calibration Curve for Hydrazine hydrate System (0-64%)

A.2: Table for plotting G.C. calibration curve

Hydrazine concentration (wt %)	*Area ratio (Water/Hydrazine)*
9.8040	13.2600
20.2000	5.6500
30.6000	2.5970
39.8800	1.8767
49.0800	1.2342
59.0000	0.8425
64.0000	0.6526

Appendix B

B.1:

Membrane: EC
Feed – Hydrazine hydrate (64 %)
Temperature: 50°C
Downstream Pressure: 0.1 mm Hg

B.1:Flux and selectivity as a function of time for a feed concentration of 64% hydrazine

Time, h	*Flux, J* $(kg/m^2.h)\ x10^3$	*Selectivity*
2	8.046	1.710
4	8.042	1.725
6	8.042	1.710
8	8.042	1.710

B.2:

Membrane: BABS1
Feed – Hydrazine hydrate (64 %)
Temperature: 50°C
Downstream Pressure: 0.1 mm Hg

B.2:Flux and selectivity as a function of time for a feed concentration of 64% hydrazine

Time, h	*Flux, J* $(kg/m^2.h)\ x10^3$	*Selectivity*
2	9.60	2.450
4	9.60	2.460
6	9.58	2.450
8	9.57	2.449

B.3:

Membrane: BABS2
Feed – Hydrazine hydrate (64 %)
Temperature: 50°C
Downstream Pressure: 0.1 mm Hg

B.3:Flux and selectivity as a function of time for a feed concentration of 64% hydrazine

Time, h	*Flux, J* $(kg/m^2.h)\ x10^3$	*Selectivity*
2	16.950	1.455
4	16.930	1.450
6	16.928	1.452
8	16.928	1.450

B.4:

Membrane: BABS3
Feed – Hydrazine hydrate (64 %)
Temperature: 50°C
Downstream Pressure: 0.1 mm Hg

B.4:Flux and selectivity as a function of time for a feed concentration of 64% hydrazine

Time, h	*Flux, J* $(kg/m^2.h)\ x10^3$	*Selectivity*
2	9.970	1.968
4	9.962	1.968
6	9.960	1.970
8	9.956	1.968

B.5:

Membrane: BABS4
Feed – Hydrazine hydrate (64 %)
Temperature: 50°C
Downstream Pressure: 0.1 mm Hg

B.5:Flux and selectivity as a function of time for a feed concentration of 64% hydrazine

Time, h	*Flux, J* $(kg/m^2.h)\ x10^3$	*Selectivity*
2	1.970	5.210
4	1.965	5.215
6	1.967	5.207
8	1.967	5.207

B.6:

Membrane: BABS5
Feed – Hydrazine hydrate (64 %)
Temperature: 50°C
Downstream Pressure: 0.1 mm Hg

B.6:Flux and selectivity as a function of time for a feed concentration of 64% hydrazine

Time, h	*Flux, J* $(kg/m^2.h) \times 10^3$	*Selectivity*
2	2.280	13.220
4	2.276	13.212
6	2.272	13.240
8	2.274	13.237

B.7:

Membrane: ABS
Feed – Hydrazine hydrate (64 %)
Temperature: 50°C
Downstream Pressure: 0.1 mm Hg

B.7:Flux and selectivity as a function of time for a feed concentration of 64% hydrazine

Time, h	*Flux, J* $(kg/m^2.h) \times 10^3$	*Selectivity*
2	5.585	4.50
4	5.585	4.50
6	5.580	4.58
8	5.763	4.58

B.8:

Membrane: MPS0
Feed – Hydrazine hydrate (64 %)
Temperature: 50°C
Downstream Pressure: 0.1 mm Hg

B.8:Flux and selectivity as a function of time for a feed concentration of 64% hydrazine

Time, h	*Flux, J* $(kg/m^2.h)\ x10^3$	*Selectivity*
2	7.300	3.050
4	7.282	3.162
6	7.282	3.160
8	7.282	3.160

B.9:

Membrane: MPS1
Feed – Hydrazine hydrate (64 %)
Temperature: 50°C
Downstream Pressure: 0.1 mm Hg

B.9:Flux and selectivity as a function of time for a feed concentration of 64% hydrazine

Time, h	*Flux, J* $(kg/m^2.h)\ x10^3$	*Selectivity*
2	9.430	2.87
4	9.425	2.87
6	9.425	2.85
8	9.425	2.87

B.10:

Membrane: MPS2
Feed – Hydrazine hydrate (64 %)
Temperature: 50°C
Downstream Pressure: 0.1 mm Hg

B.10:Flux and selectivity as a function of time for a feed concentration of 64% hydrazine

Time, h	*Flux, J* $(kg/m^2.h)\ x10^3$	*Selectivity*
2	10.410	2.520
4	10.405	2.524
6	10.402	2.523
8	10.402	2.523

B.11:

Membrane: MPS3
Feed – Hydrazine hydrate (64 %)
Temperature: 50°C
Downstream Pressure: 0.1 mm Hg

B.12:Flux and selectivity as a function of time for a feed concentration of 64% hydrazine

Time, h	*Flux, J* $(kg/m^2.h)\ x10^3$	*Selectivity*
2	11.620	1.94
4	11.630	1.93
6	11.605	1.95
8	11.591	1.97

B.12:

Membrane: MPS4
Feed – Hydrazine hydrate (64 %)
Temperature: 50°C
Downstream Pressure: 0.1 mm Hg

B.12:Flux and selectivity as a function of time for a feed concentration of 64% hydrazine

Time, h	*Flux, J* $(kg/m^2.h)\ x10^3$	*Selectivity*
2	18.340	1.240
4	18.351	1.225
6	18.320	1.237
8	18.328	1.298

Appendix

C.1: Table for calculating membrane density

Membrane	*Length (mm)*	*Width (mm)*	*Thickness (mm)*
EC	25.09	20.11	0.10
BABS1	29.19	29.62	0.08
BABS2	30.93	29.56	0.04
BABS3	30.18	25.42	0.07
BABS4	33.42	29.11	0.11
BABS5	22.65	16.21	0.06
ABS	21.47	22.59	0.21

C.2: Table for membrane density & membrane thickness

Membrane	*Membrane density (kg/m^3)*	*Thickness ($m \times 10^6$)*
EC	1004.82	60
BABS1	941.18	80
BABS2	1017.18	40
BABS3	778.36	70
BABS4	1116.67	110
BABS5	1189.32	60
ABS	950.41	75
MPS0	-	90
MPS1	-	85
MPS2	-	90
MPS3	-	85
MPS4	-	90

Appendix D

D.1: Variation of percentage sorption of water on different blended membrane

Time h	*EC (%sorption g/g of dry polymer)*	*BABS1 (%sorption g/g of dry polymer)*	*BABS2 (%sorption g/g of dry polymer)*	*BABS3 (%sorption g/g of dry polymer)*	*BABS4 (%sorption g/g of dry polymer)*	*BABS5 (%sorption g/g of dry polymer)*	*BABS6 (%sorption g/g of dry polymer)*
24.0000	4.1200	2.2000	1.1176	0.5976	1.3072	2.6730	0.3100
48.0000	4.1200	2.2000	1.1175	0.5976	1.3072	2.6730	0.3100
72.0000	4.1200	2.2000	1.1175	0.5976	1.3072	2.6730	0.3100

D.2: Variation of percentage sorption of Hydrazine hydrate on different blended membrane

Time h	*EC (%sorption g/g of dry polymer)*	*BABS1 (%sorption g/g of dry polymer)*	*BABS2 (%sorption g/g of dry polymer)*	*BABS3 (%sorption g/g of dry polymer)*	*BABS4 (%sorption g/g of dry polymer)*	*BABS5 (%sorption g/g of dry polymer)*	*BABS6 (%sorption g/g of dry polymer)*
24.0000	5.2300	4.5600	8.2100	4.8100	5.0200	5.9700	0.5000
48.0000	5.2300	4.5600	8.2100	4.8300	5.0200	5.9750	0.5000
72.0000	5.2300	4.5600	8.2100	4.8300	5.0200	5.9750	0.5000

D3: Major XRD intensity data's for various membranes

D3.1: Membrane –ABS

Intensity	*Angle°*	*d A°*
65.72	24.8	3.607919
53.01	25.75	3.459614
51.27	26.3	3.377711
67.04	27.71	3.219717
44.83	30.30	2.960009
44.25	31.08	2.877524
41.14	31.62	2.829798
40.12	31.57	2.834069
38.20	32.16	2.783689
49.80	32.84	2.727220
34.53	33.77	2.65427
32.59	34.50	2.59542

Intensity	*Angle°*	*d A°*
33.27	34.8	2.571296
34.22	35.43	2.533492
30.98	36.07	2.49023
33.53	37.00	2.429873
34.37	37.48	2.399298
32.45	38.71	2.326304
31.32	3.10	2.303930
36.72	39.68	2.271213
31.93	40.71	2.21277
34.85	41.74	2.164105
32.45	42.52	2.126087
30.09	43.55	2.078313
30.97	44.13	2.052039
33.07	45.45	1.995470

D3.2: Membrane –BABS1

Intensity	*Angle°*	*d A°*
69.07	27.65	3.226187
54.14	2.20	3.058367
49.68	30.40	2.940322
47.20	31.45	2.844510
42.48	32.00	2.796865
59.90	32.95	2.718367
38.36	33.75	2.655740
34.64	34.65	4.588793
33.98	35.35	2.539119
33.03	36.75	2.445542
34.93	37.60	2.329189
33.44	38.15	2.35858
31.05	38.65	2.329585
37.56	39.70	2.270359
33.69	41.50	2.887340
32.08	40.55	2.22470
38.25	41.70	2.165978
34.55	42.90	2.108131
34.75	43.80	2.066879
29.87	44.60	2.031646
33.96	45.55	1.91460
26.93	46.45	1.954950
26.62	49.15	1.583691

D3.3: Membrane –BABS2

Intensity	*Angle°*	*d A°*
100.00	17.89	4.958705
99.59	19.17	4.629762
88.96	20.55	4.321633
82.75	21.29	4.173093
79.41	21.78	4.079704
56.53	24.10	3.692290
61.42	25.84	3.583973
50.42	25.78	3.455768
51.72	26.17	3.404557
49.80	26.62	3.348775
81.14	27.80	3.208815
53.45	28.74	3.106271
55.20	29.53	36.025022
59.76	30.47	2.934068
53.74	31.30	2.857360
50.46	32.00	2.797247
64.90	32.98	2.715797
43.15	34.17	2.624356
40.85	34.46	2.60243
38.65	34.91	2.570404
39.49	35.45	2.532294
38.97	36.14	2.485473
40.23	40.04	2.252084
42.43	41.71	2.465333

D3.4: Membrane –BABS3

Intensity	*Angle°*	*d A°*
53.17	24.56	3.624439
54.92	25.06	3.55395
46.49	25.96	3.432254
47.47	26.61	3.350229
71.71	28.10	3.175100
47.64	29.70	3.007946
49.13	30.15	2.964160
47.91	30.85	2.898613
46.10	32.15	2.784535
59.26	33.39	2.683316
35.48	34.79	2.578694
34.64	36.04	2.492246
34.52	36.69	2.449657

Intensity	*Angle°*	*d A°*
30.99	37.43	2.402383
32.01	37.98	2.368922
30.38	38.48	2.339348
30.69	39.48	2.282488
32.55	40.08	2.249760
33.84	40.68	2.218017
32.72	41.23	2.189748
36.25	42.22	2.140277
35.16	44.07	2.054810
32.28	44.77	2.04359
31.04	46.12	1.68310

D3.5: Membrane –BABS5

Intensity	*Angle°*	*d A°*
52.42	24.65	3.611366
43.18	26.09	3.415416
41.16	26.44	3.371340
40.36	27.03	3.298440
62.42	27.78	3.211750
43.80	29.07	3.072107
46.54	30.46	2.93503
42.66	31.05	2.880170
35.72	31.65	2.827339
39.00	33.19	2.780650
49.18	32.99	2.715535
34.06	34.23	2.619925
32.33	34.77	2.580051
32.10	35.22	2.548361
33.47	41.67	2.167652

References

1) E.W. Schmidt, Hydrazine and its derivatives Preparation, Properties, Applications, John Wiely & Sons, 1984, New-York.
2) R.Q. Wilson, H.P. Munger, J.W. Clegg, Vapour-liquid equilibrium in the binary system hydrazine/water, Chemical Eng. Progr., Symp. Series 3 (1952) 115-117.
3) F. Wolf, P. Pollandt, R.Helmer, Diffusion behaviour of hydrazine through molecular sieve membranes (in German), Z.Chem.15 (1975) 160-161; Chemical Abstracts, 83,183856.
4) J.I. Dytnerskij, Membranprozesse Zur Trennung flussiger Gemische, VEB; Deutscher Verlag fur Grundstoffindustrie: Leipzig, 1977.[Cited in R. Rautenbach, R.Albrecht, "Membrane Process," John Wiely & Sons, 1989, p 368, Chichester, UK.].
5) R. Ravindra, S. Sridhar, A.A. Khan, Separation studies of hydrazine from aqueous solutions by pervaporation, J. Polymer Sci.: Part B: Polymer Physics, 37 (1999) 1969-1980.
6) M.Mulder, Basic Principles of Membrane Technology, Kulwer Academic Publishers, Dordrecht (1996).
7) R. Ravindra, S. Sridhar, A.A. Khan , A.K. Rao, Pervaporation of water, hydrazine and monomethylhydarzine using ethylcellulose membranes, Polymer, 41 (2000) 2795-2806.
8) Fuzita. H, Fortschr.Hochpolym.-Forsch., 3 (1961) 1.
9) S.V. Satyanarayana, K. Kameswararao, R. Ravindra, Prem Raj Shah, A.A. Khan. Studies on the separation of ethanol-water and hydrazine-water mixtures by pervaporation, Presented in IICT, Golden Jubilee Symposium on Advances in Chemical Engg., IICT, Hyderabad, 9-11 August 1994.
10) S.V. Satyanarayanal, P.K. Bhattacharya, Pervaporation of hydrazine hydrate: separation characteristics of membranes with hydrophilic to hydrophobic behaviour, J. Memb. Sci., 238 (2004) 103 – 115.

11) Rakesh Agrawal, Separations: Perspective of a process developer/designer, AIChE, 47 (2001) 5.

12) P. Aptel, N. Challard, J. Cuny, J. Neel, Application of the pervaporation process to the separation of azeotropic mixtures, J. Membrane Sci., 1 (1976) 271-287.

13) R. W. Baker, N. yoshioka, J.M. Mohr, A.J. Khan, Separation of organic vapours from air, J. Membrane Sci., 31 (1987) 259-271.

14) M.D.C Goncalves, D. Windmoller, N.D. M. Erismann, F. Galembeck, Pressure-driven pervaporation, Sep. Sci. Tech., 25 (1990) 1079.

15) I. Cabasso, J. Jagur-Grodzinski, D. Vofsi, A study of permeation of organic solvents through polymeric membranes based on polymeric alloys of polyphosphonates and actylcellulose. II. Separation of benzene, cyclohexene and cyclohexane, J. Appl. Poly. Sci., 18 (1974) 205-232.

16) A.C.M. Fraken, S. Ripperger, Terminology for membrane-distillation, Recommendations by the European society of membrane science and technology. Issued on Jan. 1988.

17) N. Kjellander, Design and field tests of a membrane distillation system for seawater desalination. Desalination, 61 (1987) 19-26.

18) S.F. Timashev, V.V. Valuev, R.R. Salem, A.G. Strugatshaga, Pervaporation induced by electric current, J. Membrane Sci., 91 (1994) 249.

19) J. Neel, P. Aptel, and R. Clement, Desalination, 53 (1985) 297-396.

20) P.A. Kober, Pervaporation, Perstillation, and Percrystallisation, J. of Amer. Chem. Soc., 39 (1917), 9444.

21) L. Kahlenberg, On the nature of the process of osmosis and osmotic pressure with observations concerning dialysis. J. Phys. Chem., 10 (1906) 141.

22) L. Farber, Applications of pervaporation, Science 82 (1935) 158.

23) E.G. Heisler, A.S. Hunter, J. Sicilliano, R.H. Treadway, Solute and temperature effects in the pervaporation of aqueous alcoholic solutions. Science, 124 (1956) 77.

24) R.C. Binning, R.J. Lee, J.F. Jenning, E.C. Martin, Separation of liquid mixtures by pervaporation. Ind. Eng. Chem, 53 (1961) 45-50.

25) R.C. Binning, F.E. James, How to separate by membrane permeation. Petroleum Refiner, 37 (5) (1958) 214-215.

26) H.E.A. Bruschke, W.H. Schneider, G.F. Tusel, Pervaporation membrane for the separation of water and oxygen containing simple organic solvents. Communication, European workshop on pervaporation, Nancy, France, Sept. 21-22, 1982.

27) A.Jonquières, R. Clément, P. Lochon, J. Néel, M. Dresch, B. Chrétien, Industrial state-of-art of pervaporation and vapour permeation in the western countries, J. Membr. Sci. 206, (2002) 87-117.

28) X. Feng, R.Y.M. Huang, Liquid separation by membrane pervaporation: A review, Ind. Eng. Chem. Res. 36 (1997) 1048-1066.

29) J.L. Bravo, J.R Fair, J.L. Humphery, C.L. Martin, A.F. S. Seibert, Fluid mixture separation technologies for cost reduction and process improvement, Noyes Data: Park Ridge, NJ, 1986.

30) R. Baker, Membrane technology in the chemical industry: Future Directions. In: Membrane technology in the chemical industry, Edited by S.P. Nunes and K.-V. Peinemann, Wiley-VCH, Verlag Gmbh, Weinheim, 2001.

31) F. W. Greenlaw, R. A, Shelden and E. V. Thompson, "Dependence of Diffusive Permeation Rates on Upstream and Downstream Pressures. II. Two Component Permeant," J. Memb. Sci., **2**, 333 (1977).

32) J. P. Brun, C. Larchet, R. Melet and G. Bulvestre, "Modeling of Pervaporation of Binary Mixtures through Moderately Swelling, Non Reacting Membranes," J. Memb. Sci., **23**, 257 (1985).

33) C. K, Yeom and R. Y. M. Huang, "Modeling of Pervaporation Separation of Ethanol-Water Mixtures through Cross-linked Poly(vinyl alcohol) Membrane," J. Memb. Sci., **67**, 39 (1992).

34) P. J. Flory, Principles of Polymer Chemistry, Cornell University Press, Ithaca, New York (1953).

35) Tomoyuki Okada and Takeshi Matsuura, "A New Transport Model for Pervaporation," J. Memb. Sci., **59**, 133 (1991).

36) Jyh-Jeng Shieh and Robert Y. M. Huang, "A Pseudophase Change Solution Diffusion Model for Pervaporation. i. Single Component Permeation," Sep. Sci. Tech., **33(6)**, 767 (1998).

37) M B. Ewing, T. H. Lilley, G.M. Olofsson, M. T. Rätzsch and G. Somsen, "IUPAC: A Report of IUPAC Commission I.2 on Thermodynamics: Standard Quantities in Chemical Thermodynamics. Fugacities, Activities, and Equilibrium Constants for Pure and Mixed Phases," J. Chem. Thermodynamics, **27**, 1 (1995).

38) Paul D.R. and Ebra – Lima O.M.: Mechanism of liquid transport through swollen polymer membranes. J. Appl. Polym. Sci. 15, 2199 (1971).

39) Paul D.R. and Paciotti J.D.: Drivining force for hydraulic and pervaporative transport in homogeneous membranes. J. Polym. Sci. Polym. Phys .Ed .13 1201 (1975).

40) McCandless F.P.: Separation of aromatics and napthenes by permeation through modified vinylidene fluoride films. Ind. Eng. Chem. Proc. Des. Develop. 12, 354 (1973)

41) Sikonia J.G. and McCandless F.P. Separation of isomeric xylenes by permeation through modified plastic films. J. Memb. Sci. 4, 229 (1978).

42) Mulder M.H.V. Kruitz F. and Smolders C.A.: Separation of isomeric xylenes by pervaporation through cellulose ester membranes. J. Memb. Sci. 11, 349 (1982).

43) Hansen C. and BEErbower A.: Kirk-Othmer, Ency. Of Chem. Tech., Supplement Vol. p 889

44) Y.C Jean., Characterizing free volumes and holes in polymers by positron annihilation spectroscopy, NATO Advanced Research Workshop, Advances with Positron Spectroscopy of Solids and Surfaces, Varenna, Italy, July 16-17,1993.

45) S.J. Tao, Positronium annihilation in molecular substances, J. Chem. Phys., 56 (1972) 5499-5510.

46) M .Eldrup, D. Lightbody, J.N. Sherwood, The temperature dependence of positron lifetimes in solid pivalic acid, Chem. Phys., 63 (1981) 51-58.

47) H. Nakanishi, S.J. Wang, Y.C. Jean, in S.C. Sharma, (Ed.), Positron annihilation studies of fluids, World Scientific, Singapore, 1988. p.292.

48) A.J. Hill, S. Weinhold, G.M. Stack, M.R. Tant, Eur Polym J., 32 (1996) 843.

49) K. Ciesielski, A.L. Dawidowicz, T. Goworek, B. Jasinska, J. Wawryszczuk, Positronium lifetimes in porous vycor glass, Chem. Phys. Lett. 289 (1998) 41-45.

50) G. Akovali and A. Ozkan : Notes on modification of polystyrene by sulphonation: Some properties of Poly(styrenesulphonic acid), Polymer , 27 1277-1280 (1986).

51) R.A. Penneman, L.F. Audrieth, Quantitative determination of hydrazine, Analytical Chemistry, 20 (1948) 1058-1061.

52) L.A. Dee, A.K. Webb, Gas chromatographic separation of hydrazine mixtures and water using a stationary phase that is chemically similar to hydrazine, Anal. Chem. 39 (1967) 1165-1167.

53) A. Hillaire, E. Favre, Isothermal and nonisothermal permeation of an organic vapour through a dense polymer membrane, Ind. Eng. Chem. Res. 38 (1999) 211-217

54) Lee CH. J Appl Polym Sci., 19, 83 (1975).

55) J.G. Wijmans, R.W. Baker, The solution–diffusion model: a review, J. Membr. Sci., 107 1-21, (1995).

56) Bode E, Busse M, Ruthenberg K. J Membr Sci., 77, 69 (1993).

57) Cote J, Lipski C. Proceedings of the Third International Conferenceon Pervaporation Process in the Chemical Industry. Nancy, France,September, 19–22, 1988. p.449.

58) P. Kirkegaard, N.J. Pedersen, M. Eldrup, PATFIT-88: a data processing system for positron annihilation spectra on mainframe and personal Computers, Riso National Laboratory, Denmark, 1989.

59) L.H. Sperling, Introduction to Physical Polymer Science; John Wiley Publishers: New-York, 1986

60) Jin Chuan Yang, Michael J. Jablonsky, Jimmy W. Mays, NMR and FT-IR studies of sulphonated syrene-based homopolymers and copolymers, Polymer 43 5125-5132 (2002).

61) Orler EB, Yontz DJ, Moore RB. Macromolecules ,26, 5157-60 (1993).

62) Zundel G., Hydration and intermolecular interaction. New York: Academic Press; 1969.